



Quality of Service Evaluation of LiFi-Based Transmission: Simulation and Performance Analysis

A Project submitted in partial fulfillment of the requirements for the degree of Bachelor of Science (B.Sc) in Computer Networks & Communications.

By

Bushra Mustafa Yousef (3013)

Supervisor

Mr. Mohamed Elshatshat

Copyrights © 2020.

All rights reserved, no part of this project work may be reproduced in any form, or by any means, without the permission in writing from the author(s) and the department of Computer Networks & Communications, Faculty of IT, University of Benghazi.

Abbreviation

AP Access Point

APD Avalanche Photodiode Detector

AWGN Additive White Gaussian Noise

ACO-OFDM Asymmetrically Clipped Optical OFDM

BS Base station

BER Bit Error Ratio

CIM Color Intensity Modulation

CIR Channel Impulse Response

CSMA-CA Carrier Sense Multiple Access-Collision Avoidance

CSK Color-Shift Keying

DC Direct Current

DD Direct Detection

DCO-OFDM Direct Current Optical-Orthogonal Frequency Division Multiplexing

E_b/N_0 Energy per bit-to-noise power-spectral-density ratio

FDM Frequency Division Multiplexing

FOV Field of View

FSO Free Space Optical

HFRFT Higher Frequency Reuse Factor-based Transmission

IOT Internet of Things

IM Intensity Modulation

IR Infrared

LD Laser Diode

IFFT Inverse Fast Fourier Transform

ISI Inter Symbol Interference

IM-DD Intensity Modulation Direct Detection

Li-Fi Light Fidelity

LD Laser Diodes

LOS Line Of Site

LED Light Emitting Diode

MPWM Multi-way Pulse Width Modulation (PWM)

MPR Multi-packet Reception

MSE Mean squared error

MT Mobile Terminal

MIMO Multiple Input-Multiple Output

MPWM Multi-Way Pulse Width Modulation

MPPM Multi-path Pulse Position Modulation

MCM Multi-Carrier Modulation

MM Metameric Modulation

MAC Media Access Control

OWC Optical Wireless Communication

OOK On-Off Keying

OFDM Orthogonal Frequency Division Multiplexing

OW Optical Wireless

PSNR Peak Signal to noise Ratio (SNR)

PWM Pulse Width Modulation

POE Power Over Ethernet

PIN p-intrinsic-n

PPM Pulse Position Modulation

PAM Pulse Amplitude Modulation

PD Photo diodes

PHY Physical

PAM-DMT Pulse Amplitude Modulation-

PC Phosphor Coated

QOS Quality Of Service

QAM Quadrature Amplitude Modulation

QPSK Quadrature Phase Shift Keying

RF Radio Frequency

RB Resource Blocks

SNR Signal to noise Ratio

SDN Software-Defined Networking

SLER Slot Error Rate

TIA Trans Impedance Amplifier

UFR Unity Frequency Reuse

UV Ultra Violet

VLC Visible Light Communication

VPPM Variable Pulse Position Modulation (PPM)

VT Vectored Transmission

Wi-Fi Wireless Fidelity.

4 System Model and Simulation	23
4.1 Introduction	24
4.2 System Model:	24
4.3 Simulation Algorithm and Parameters:	25
4.4 Channel Modeling:	26
4.4.1 Transmitter:	27
4.4.2 Line of Sight Line Of Site (LOS) channel model:	28
4.4.3 Receiver:	29
4.4.4 Noise:	30
4.4.5 Signal to Noise Ratio (SNR):	31

CONTENTS

4.5 Modulation:	32
4.5.1 On-Off-keying (OOK):	32
4.5.2 Pulse Position Modulation (PPM):	33
4.5.3 Quadrature Amplitude Modulation (QAM)	34
4.5.4 Quadrature Phase Shift Keying (QPSK)	35
4.6 Quality of Service (QOS) Indicators	35
4.6.1 Bit Error Ratio (BER)	35
4.6.2 Mean Squared Error MSE	36
4.7 Summary	36
5 Results and Discussion	37
5.1 Introduction:	38
5.2 Signal Distribution:	38
5.3 Modulation type versus BER:	39
5.3.1 Bit Error Rate and E_b/N_0 for OOK :	39
5.3.2 Bit Error Rate/Slot Error Rate of L-PPM :	42
5.3.3 Comparison Between Different PPM and OOK Schemes	46
5.4 Image transmission using Quadrature Amplitude Modulation (QAM) and Quadrature Phase Shift Keying (QPSK) modulation:	48
5.5 Summary	53
6 Conclusion and Future Work	55
6.1 Conclusion	56
6.2 Future Work	56
References	56

List of Figures

4.1	A system block diagram of a Li-Fi system.	25
4.2	Model of the OWC in time domain.	27
4.3	Geometry of LOS propagation model.	29
4.4	pulsed modulation schemes, OOK and PPM.	33
4.5	16-QAM modulation.	34
4.6	64-QAM modulation.	34
4.7	QPSK Modulation	35
5.1	Received power 20mw	38
5.2	The optical channel gain	39
5.3	Bit error curve for On-Off Keying (OOK) modulation ,using power 20mw	40
5.4	BER to E_b/N_0 for OOK modulation, using power 20mw	40
5.5	Bit error curve for OOK modulation , (power 10 mw)	41
5.6	BER to E_b/N_0 for OOK modulation, (power 10 mw)	41
5.7	Bit error rate curve for 8-PPM modulation ,(power 20 mw)	42
5.8	Bit error rate curve for 16-PPM modulation , (power 20 mw)	42

5.9	Bit error rate curve for 32-PPM modulation, (power 20 mw)	43
5.10	Bit error rate curve for 64-PPM modulation , (power 20 mw)	43
5.11	Bit error rate curve for 8-PPM modulation, (power 10 mw)	44
5.12	Bit error rate curve for 16-PPM modulation, (power 10 mw)	44
5.13	Bit error rate curve for 32-PPM modulation , (power 10 mw)	45
5.14	Bit error rate curve for 64-PPM modulation , (power 10 mw)	45
5.15	Slot error rate curve for L-PPM modulation, (power 10 mw)	46
5.16	Slot error rate curve for L-PPM modulation, (power 20 mw)	46
5.17	Difference between power in SLER for 64-PPM modulation	47
5.18	Difference between power in BER for OOK modulation	47
5.19	Original image before transmission	48
5.20	Transmission the image using 16-QAM modulation, (power 20 mw)	49
5.21	Transmission the image using 64-QAM modulation, (power 20 mw)	49
5.22	Transmission the image using 16-QPSK modulation, (power 20 mw)	50
5.23	Mean Squared Error (Power 20 mw)	50
5.24	transmission the image using 16-QAM modulation, (power 10 mw)	51
5.25	transmission the image using 64-QAM modulation, (power 10 mw)	51
5.26	transmission the image using 16-QPSK modulation, (power 10 mw)	52
5.27	Mean Squared Error, (power 10 mw)	52

List of Tables

4.1 System Parameters for a Li-Fi Link	26
--	----

Abstract

As a wireless connectivity solution with low latency and high capacity, visible light communication (VLC) is particularly attractive for high-speed applications such as an image or real-time video transmission. Light-Fidelity (Li-Fi) is an emerging technology for wireless optical networking using the concept of Visible light communication (VLC). The development of a Light-emitting diode (LED) brought extraordinary progression in which visible light communication is performed. LEDs can be used for transmitting the information. VLC uses LED as the transmitter which sends information by blinking the light which will be unnoticeable to the natural eyes. This project aims to learn about Li-Fi technology and perform simulations using MATLAB for performance analysis, with the use simple line of sight (LOS) channel model is possible to understand, how the optical power distribution in a LOS path through the room. Also, calculating the quality of service (QOS) when sending a random-signal using two modulations On-Off-keying (OOK) and Pulse Position Modulation (L-PPM) through the Bit Error Ratio (BER) function, and the Mean squared error (MSE) function when sending the image using two modulation Quadrature amplitude modulation (QAM) and Quadrature Phase Shift Keying (QPSK)

Key Word: Light-fidelity, Visible light communication, Light Emitting Diode , line of sight, Mean squared error, Quadrature Phase Shift Keying, Quadrature amplitude modulation, Pulse Position Modulation, On-Off-keying, Bit Error Ratio.

Chapter 4

System Model and Simulation

4.1 Introduction

In order to study the performance of Li-Fi systems, for which the theory was portrayed in the past parts, we played out some simulations. In general, a simulation is a rearranged model of reality wherein the emphasis is on what are accepted to be the predominant phenomena and second-order impacts can be abandoned.

This model, as a rule, is converted into a Phosphor Coated (PC) algorithm that is capable of a limited number of steps to compute the parameters that we need to assess. For our simulations, we chose to use the MATLAB program since it is well-known programming with a tool kit pack (like Bit Error Ratio (BER) function) fit a communication system. Moreover, numerous Li-Fi research elements use MATLAB algorithms.

4.2 System Model:

To Li-Fi simulation, The LOS block is the most important block in the Li-Fi system. The channel represents how the transmitter light ray moves through space to arrive at the receiver. The main component to analyze Li-Fi channels is the LOS transmission.

Many typologies are normally used for indoor applications. The arrangements can be characterized by, the level of the directionality of transmitters, receivers, and the presence of the LOS way between the transmitter and the receiver.

IM-DD is the accepted strategy for executing optical wireless systems chiefly because of its diminished expense and complexity. In the IM-DD, Li-Fi system, the drive current LED of an optical source is legitimately balanced by the adjusting signal, which thus fluctuates the intensity of the optical source, i.e., the communicated optical force is corresponding to LED.

The recipient used a photo-detector, with a reaction, which is the mix of a huge number of short frequencies of the episode optical sign, that creates a photo-current. This photo-current is legitimately corresponding to the prompt optical force occurrence upon it.

That is, the photo-current is corresponding to the square of the got electric field. An IM-DD -the based optical wireless system has a comparable base-band model that shrouds the high-recurrence nature of the optical transporter [13].

The area of the system and, the general condition is the primary components to be viewed as examining Li-Fi innovation. Li-Fi isn't appropriate for significant distance correspondence in

light of the fact that the sent sign can't pass the misty articles (for example, dividers, structures, and so on...).

The way that the Li-Fi signal doesn't infiltrate dividers isn't just a negative property since this allows the sign to be restricted in a shut room. This limit encourages security techniques. The second thought about the system area is that the Li-Fi system depends on light force balance. Then, each natural light might be the reason for genuine impedance.

The Li-Fi light can give brightening to the general condition. The simplest condition to investigate and reproduce is an instance of a short-range, indoor, shut room, system. Likewise, a shut room can be unfilled or loaded up with furniture and windows. (in this project, the room is empty).

It relies upon how one needs the system to be precise and relies upon what number of computation assets one has accessible. The system simply portrayed will be broken down later in detail. See the Li-Fi system Diagram in Fig. (4.1).

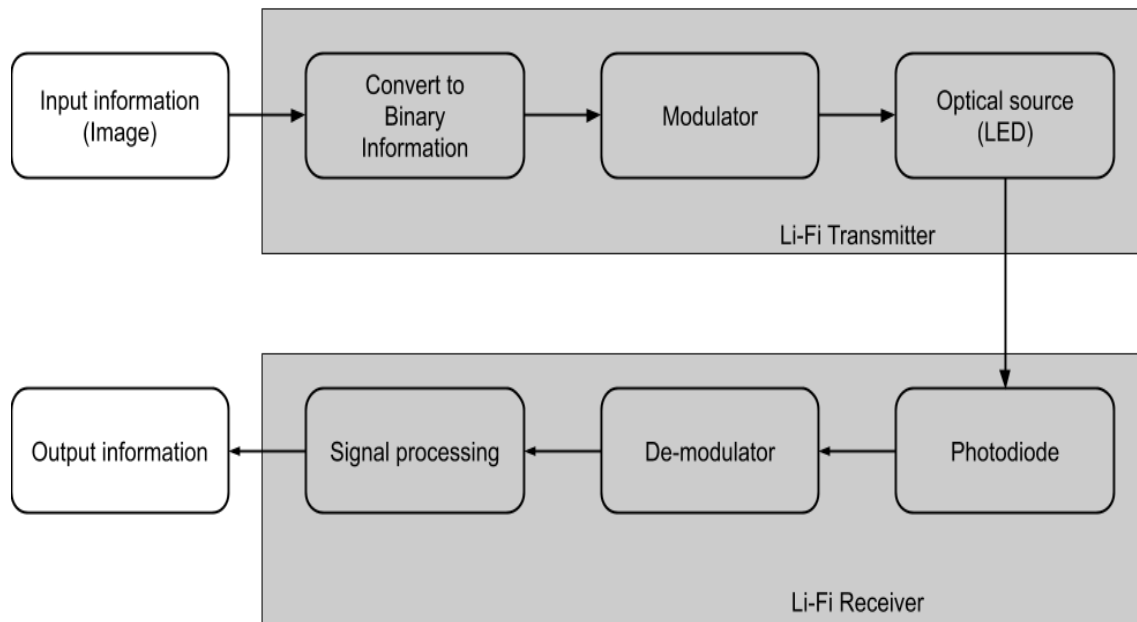


Figure 4.1: A system block diagram of a Li-Fi system.

4.3 Simulation Algorithm and Parameters:

In this section, a table of the parameters used in simulation and a logarithm to explain the simulation method. The table (4.1) shows the parameters used in the simulation,

Table 4.1: System Parameters for a Li-Fi Link

	Parameters	Value
Room	Size	5*5*3 m
	Reflection coefficient	0.8
Receiver	Responsivity of receiver	0.6
	Half-angle FOV	30°
source	Active area (Receiver)	7.8E-7
	Receiver height	1.45
source	Semi-angle at half power	60°
	Transmit power (per LED)	20 mw
Noise	Led position is ceiling centre	(0,0,0)
	Noise bandwidth factor	0.562
Optical filter	Ambient light power	7E-8 A
	Mplifier noise density	5e-12 A/Hz
A lens at the PD	Amplifier bandwidth	4.5E6 Hz
	Electron charge	1.60E-19
A lens at the PD	Data rate	11500
	Gine	1
A lens at the PD	Refractive index	1.5
PPM Modulation parameters		
	Bit	3,4,5,6
	Slot rate symbol rate	200
	number of PPM symbols	1e6

and the implemented Li-Fi algorithm is presented in Algorithm (1).

4.4 Channel Modeling:

The optical wireless channel has been demonstrated to be a direct, time-invariant, memory-less system with an impulse reaction of limited duration. The summed up model of the OWC link in the time domain is delineated in (4.2) [12].

Algorithm 1 Li-Fi

```

1: Initialization: input the Parameters in table 4.1.
2: Calculate the distribution of the optical radiation by, (4.1) (4.2) (4.4).
3: Calculate the power of LOS by (4.3).
4: Calculate the noise by (4.6), (4.7), (4.8).
5: Calculate the SNR by (4.9).
6:  $SNR_{db} = 10 \log_{10}(SNR)$ .
7: Calculate the  $E_b/N_o$  by (4.13).
8: for  $i \in \{1, \dots, T\}$  do
9:   Calculate the PPM by (4.15).
10:   $L_{sy} = 2B_o$ .
11:  for  $j \in \{1, \dots, SNR_{db}\}$  do
12:    Calculate  $S_{gma}, P_{pg}$  by (4.12),  $I_{peak}$  by (4.11),  $E_{peak}$  by (4.10).
13:    Calculate BER by ().
14:  end for
15: end for
16: for  $i \in \{1, \dots, T\}$  do
17:   Calculate the OOK by (4.14).
18:   for  $j \in \{1, \dots, SNR_{db}\}$  do
19:     Calculate  $S_{gma}, P_{pg}$  by (4.12),  $I_{peak}$  by (4.11),  $E_{peak}$  by (4.10).
20:     Calculate BER by (4.22).
21:   end for
22: end for
23: Process the images.
24: for  $i \in \{16, \dots, X, \text{ where } i = 2L\}$  do
25:   Calculate the QAM by (4.16, 4.17, 4.18, 4.19, 4.20).
26:   Calculate the MSE by (4.23).
27: end for
28: Calculate the QPSK by (4.21).
      Calculate MSE by (4.23).

```

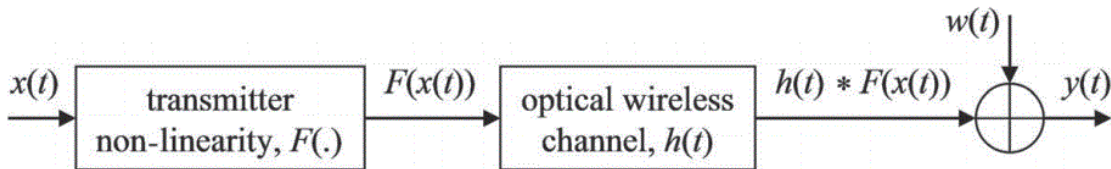


Figure 4.2: Model of the OWC in time domain.

4.4.1 Transmitter:

The angular distribution of the optical radiation could be defined by Lambertian radiant intensity by (4.1) [12].

$$R_0(\phi) = \begin{cases} \frac{(m+1)}{2\pi} \cos^m(\phi) & \text{if } \phi \in [-\frac{\pi}{2}, \frac{\pi}{2}] \\ 0 & \text{for } \phi \geq \frac{\pi}{2} \end{cases} \quad (4.1)$$

Where :

m : is Lambert's model number expressing directivity of the source beam (4.2).

ϕ : Is the angle of maximum radiated power. The order of Lambertian emission m is related to the LED semi angle at half-power.

$\phi_{\frac{1}{2}}$: Transmitter Semi-angle, angle of irradiance in half

Lambert radiator is a typical radiation model, and a LED light source in VLCs can be approximated to a Lambert radiator. Order of Lambertian emission by [12] (4.2):

$$m = \frac{-\ln 2}{\ln \cos(\phi_{\frac{1}{2}})} \quad (4.2)$$

4.4.2 Line of Sight LOS channel model:

In short-distance LOS links, multi-path dispersion is seldom a problem and LOS links channel is often modeled as a linear attenuation and delay.

The optical channel gain in indoor scenarios consists of the line of sight LOS component and the multi-path reflections. The LOS channel gain is expressed as in [2] this can be explained in Fig. (4.3) [12].

The channel gain of the LOS channel from the LED source (4.3):

$$H_{\text{LOS}} = \begin{cases} \frac{A}{d^2} \cos(\phi_{\frac{1}{2}}) T_s(\Psi) g(\Psi) R_0 & 0 \leq \psi \leq \Psi_c \\ 0 & \text{elseWhere} \end{cases} \quad (4.3)$$

The optical gain of an ideal non-imaging concentrator having internal refractive index n is Where (4.4) [12].

$$g(\psi) = \begin{cases} \frac{n^2}{\sin^2 \Psi_c} & 0 \leq \psi \leq \Psi_c \\ 0 & \psi > \Psi_c \end{cases} \quad (4.4)$$

A: The area of the receiver photodiode.

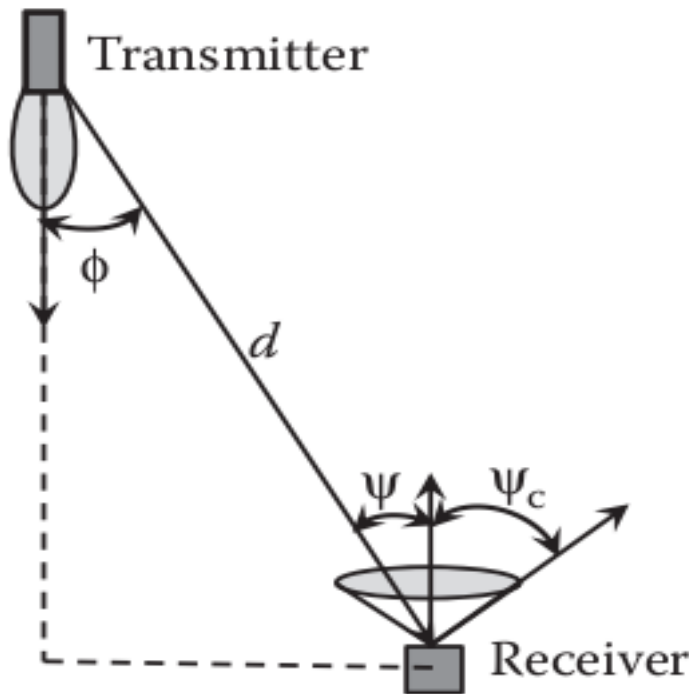


Figure 4.3: Geometry of LOS propagation model.

d: Distanciation between Tx and Rx.

ϕ : The angle between the LED normal and d.

$T_s(\Psi)$: Gain of an optical filter

$\Psi_c \frac{\pi}{2}$: The Field of View (FOV) From the constant radiance theorem.

n: Is the refractive index.

4.4.3 Receiver:

They read the flashing patterns of LED and construe them as information [21].

To make a full-duplex communication, the versatile terminal utilizes IR transmission to talk with closest optical APs. Different analyses of adding the two emitters and PD properties are in progress [23].

optical power to obtain the power on the receivers (4.5) [12].

$$P_r = H_{\text{LOS}} P_t g(\psi) T_s \quad (4.5)$$

Where :

P_t : The transmitted power.

4.4.4 Noise:

An optical communication system can be affected by many noise sources. To obtain fully-fledged SNR definition, these sources should be investigated carefully. These are the noise: (photon fluctuation noise, dark current, excess noise, and thermal noise).

For fiber optical communication systems, however, background radiation noise can be neglected since optic beams are isolated from the background [12].

- **Quantum Shot Noise:**

Shot-noise is come about because of the molecule characteristic of photons. For an occurrence light with steady power, the quantity of approaching photons per unit time vacillates with a Poisson dispersion. In the event that the quantity of photons that the PD finder got per unit time is sufficiently huge, the shot commotion can be displayed as an added Additive White Gaussian Noise (AWGN).

The fluctuation of the shot noise is relative to the optical power received by the PD finder. In any case, optical power received is overwhelmed by the steady background light and the DC component of the signal.

Thus, the shifting of the shot noise difference is insignificant, and the shot noise is accepted to follow a Gaussian conveyance with zero mean and a fluctuation of Q^2 shot = N_0 , shot F_s . The parameter F_s represents the modulation bandwidth [13].

The quantum shot noise is given by (4.6) [12] :

$$S_q(\omega) = q\langle i \rangle \quad (4.6)$$

The shot-noise is given by (4.7) [12]:

$$Q_q^2 = 2q\langle i \rangle B_{ef} \quad (4.7)$$

Where:

q = The electron charge.

$\langle i \rangle$ = Is the mean current of arrival signal.

B_{ef} = The noise frequency bandwidth.

- **Thermal noise:**

Another receiver noise is named thermal noise. Thermal noise is fundamental because of the temperature variance brought about by the resistive units in the receiver circuit.

In a large portion of the optical receiver, Trans Impedance Amplifier (TIA) is incorporated to enhance the got signal. The resistance of the TIA is a significant wellspring of thermal noise (4.8) [13].

$$\langle i_T^2 \rangle = 4K_B \frac{T B}{R_L} \quad (4.8)$$

4.4.5 Signal to Noise Ratio (SNR):

SNR is the ratio of signal strength to noise power. This dimensionless quantity is a very important parameter for all communication systems. It is a kind of quality factor of a communication system. If the SNR is low, the system is not transmitting correctly.

It is desirable to have the highest possible SNR. However, this means an increase in system costs, because an increase in signal strength means higher power consumption and a decrease means an increase in noise power system complexity. Usually, the center channel is the best option. The SNR has to be as high as possible to transmit it properly, but most be low enough to keep system costs down the SNR is given by (4.9) [12]:

$$SNR = \frac{(RP_r)^2}{\text{Total Noise}} \quad (4.9)$$

Where:

R : is the PD responsivity.

P_r : is the received power.

Noise : Total Noise (Quantum Shot Noise , Thermal noise ... etc).

4.5 Modulation:

4.5.1 On-Off-keying (OOK):

OOK dimming can be achieved by refining the ON/OFF levels and applying for symbol compensation.

Dimming through refining the ON/OFF levels of the LED can maintain the same data rate, however, the reliable communication range would decrease at low dimming levels. On the other hand, dimming by symbol compensation can be achieved by inserting additional ON/OFF pulses whose duration is determined by the desired dimming level [24]. As shown in the Fig. (4.4). The electrical power and the peak and bit energy for one period of (4.10).

$$E_{\text{peak}} = I_{\text{peak}}^2 T_b \quad (4.10)$$

(4.10) Peak power and energy peak and bit for one period.

E_{peak} :The energy peak of the triangular wave.

$$I_{\text{peak}} = 2RP_{\text{avg-ook}} \quad (4.11)$$

I_{peak} =The peak wave current.

R =The photodiode responsivity.

$$P_{\text{avg}} = \sqrt{\frac{(noise R_b E_b/N_0)^2}{2 R_{\text{rx}}}} \quad (4.12)$$

Where:

R_b : Bit rate.

$$E_b/N_0 = 10^{10 \log \text{SNR}/10} \quad (4.13)$$

OOK is the most reported modulation techniques for IM-DD in optical communication. The envelop for OOK is given by a (4.14) :

$$p(t) == \begin{cases} 2P_r & \text{for } t \in [0, T_b) \\ 0 & \text{elsewhere} \end{cases} \quad (4.14)$$

Where

P_r : the average power.

T_b : the bit duration.

4.5.2 Pulse Position Modulation (PPM):

Single-pulse position modulation (L-PPM) alludes to a period of time that is divided into a few time allotments, and afterward, a solitary pulse signal is sent at one schedule opening for information transmission. Single-pulse position modulation can be depicted as planning n-bit double information to a solitary pulse signal at a specific schedule opening time of the $N^{1/4} 2^n$ time allotments [25]. This can be explained in Fig. (4.4).

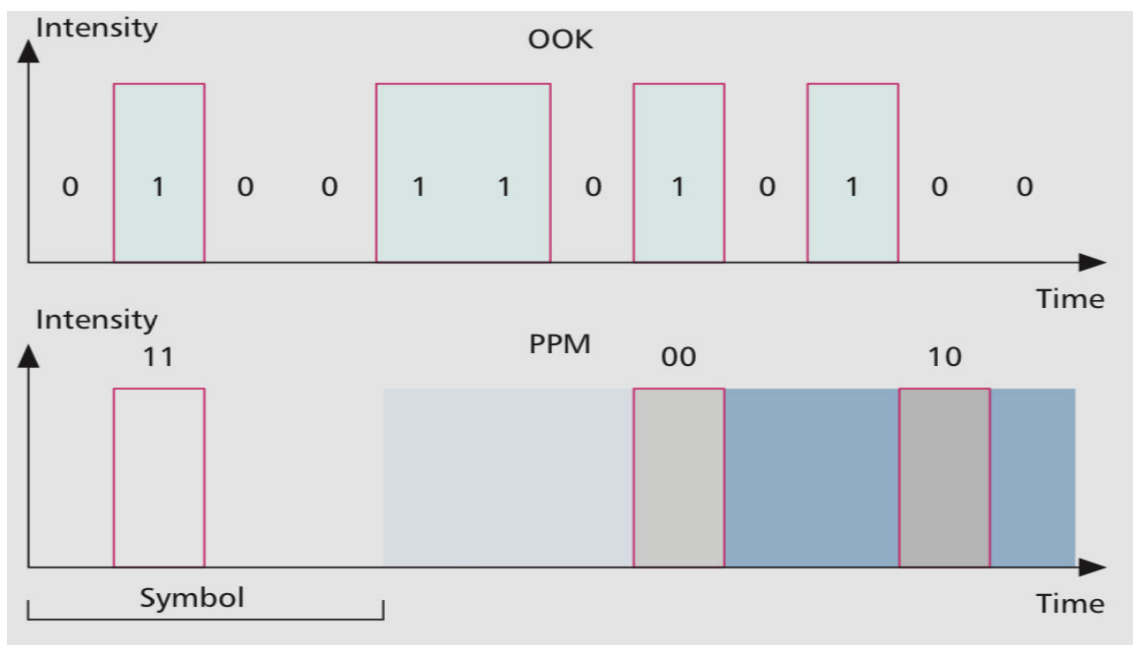


Figure 4.4: pulsed modulation schemes, OOK and PPM.

Compared with OOK, PPM is more power-efficient but has lower spectral efficiency. A variant of PPM, termed Variable PPM (VPPM), can provide dimming support by changing the width of signal pulses, according to a specified brightness level. Therefore, VPPM can be viewed as a combination of PPM, the PPM is given by a (4.15) [24].

$$x(t)_{\text{PPM}} = \begin{cases} 1 & , \text{for } t \in [(m-1)T_{s,\text{ppm}}, mT_{s,\text{ppm}}] \\ 0 & \text{elsewhere} \end{cases} \quad (4.15)$$

Where:

$$m \in \{1, 2, \dots, L\}.$$

L: bit resolution $M > 0$ is an integer.

T_s = pulse of one slot duration .

4.5.3 Quadrature Amplitude Modulation (QAM)

QAM is defined as modulation technology and is a combination of phase and amplitude modulation of the carrier wave in a single channel. QAM has been widely used in the modification due to its efficiency in power and bandwidth [26].

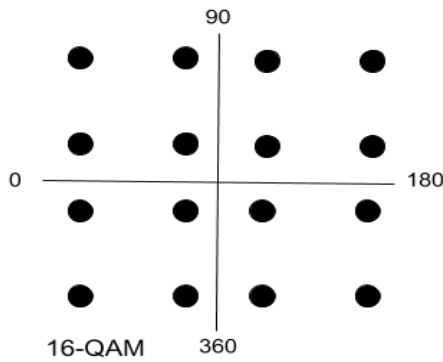


Figure 4.5: 16-QAM modulation.

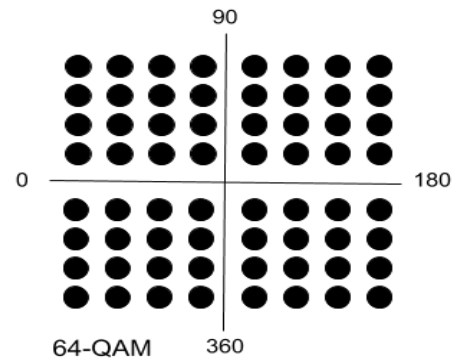


Figure 4.6: 64-QAM modulation.

The input signals to the low-pass filter are given by (4.16), (4.17), and (4.18) [12]:

$$r_1(t)_{\text{QAM}} = I(t)\cos^2(w_c t) - \cos(w_c t) \quad (4.16)$$

$$r_1(t)_{\text{QAM}} = 0.5I(t)0.5\cos^2(2w_c t) - 0.5\cos(2w_c t) \quad (4.17)$$

$$r_Q(t)_{\text{QAM}} = 0.5I(t)[\sin(2w_c t) + 1 - \cos(2w_c t)] \quad (4.18)$$

If the carrier at the Rx has a small frequency error Δw (but a phase error $\theta = 0$), then the two output signals are given as (4.19), (4.20) [12]:

$$r_{I-0}(t)_{\text{QAM}} = 0.5I(t)[1 - \cos^2(\Delta w_c t) - \sin(\Delta w_c t)] \quad (4.19)$$

$$r_{I-0}(t)_{\text{QAM}} = 0.5I(t)[\sin^2(\Delta w_c t) + 1 - \cos(\Delta w_c t)] \quad (4.20)$$

4.5.4 Quadrature Phase Shift Keying (QPSK)

QPSK is the most commonly used modulation system in a modern digital communication system, providing high performance on bandwidth efficiency and bit error rate (4.7) [27].

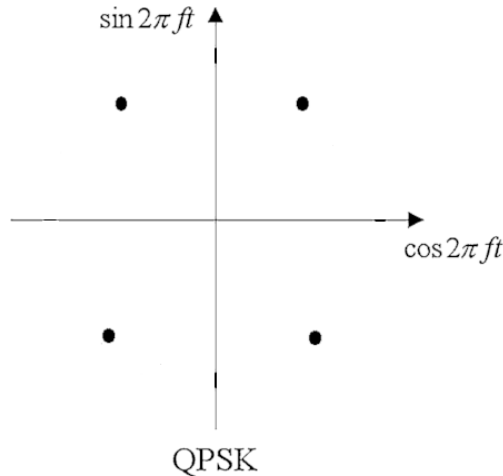


Figure 4.7: QPSK Modulation

$$QPSK = \cos(wt + (2m - 1)\frac{\pi}{4}) \quad (4.21)$$

4.6 Quality of Service (QOS) Indicators

Quality is a significant parameter for all signal and their functionalities. picture quality is a prime model. For original image quality assessment, ground truth is required. but, it is hard to find the ground truth. As a rule, in general, quality is being evaluated by full reference measurements.

4.6.1 Bit Error Ratio (BER)

In Communication, BER is significant on the grounds that is a perfect parameter to appraise the quality of the communication system. The ratio of how many bits received in error over the number of total bits received is the BER.

This measured ratio is affected by many factors including signal to noise and distortion. Widely used modulation techniques in Li-Fi technology are OOK, PPM, Pulse Amplitude Modulation (PAM) as demonstrated in [21]. Typically this boundary can be assessed with

simulation or with theoretical analytical calculations [12].

The probability of error is given as (4.22) [12]:

$$BER = \frac{N_{\text{Err}}}{N_{\text{Bit}}} \quad (4.22)$$

Where:

N_{Err} : Number of Error.

N_{Bit} : Number of bits.

4.6.2 Mean Squared Error MSE

Mean squared error (MSE) is the most widely recognized assessor of picture quality estimation metric. It is full reference values and the qualities more like zero is the better. The MSE measures the average of the square of the errors.

The error is the dispute between the estimator and predestined outcome as $g(x, y)$ and $g^{(x,y)}$ is defined as (4.23) [28]:

$$\text{MSE} = \frac{1}{NM} \sum_{j=1}^M \sum_{i=1}^N (Y_{i,j}, X_{i,j})^2 \quad (4.23)$$

Where : M and N length the i and j.

4.7 Summary

System implementation is the most important part of this project, as there are many components and requirements for this implementation. Defining how the system model and simulations should be built and components, ensuring that the codes are operational and used each is described in this chapter.

Chapter 5

Results and Discussion

5.1 Introduction:

In this chapter, our related work on this project as a simulation and the obtained results using MATLAB. The values in Table 4.1, were used for simulation.

Each section contains simulation results, some enhancement, and discussion concerning the results. The following topics we will discuss BER, Signal Distribution, and transmission images.

5.2 Signal Distribution:

The optical power distribution for a receiver plane in a LOS path, ignoring the reflection of walls, shown in Fig. 5.1 for one transmitter in the room ($5 \times 5 \times 3$), and Fig. 5.2 for the optical channel gain.

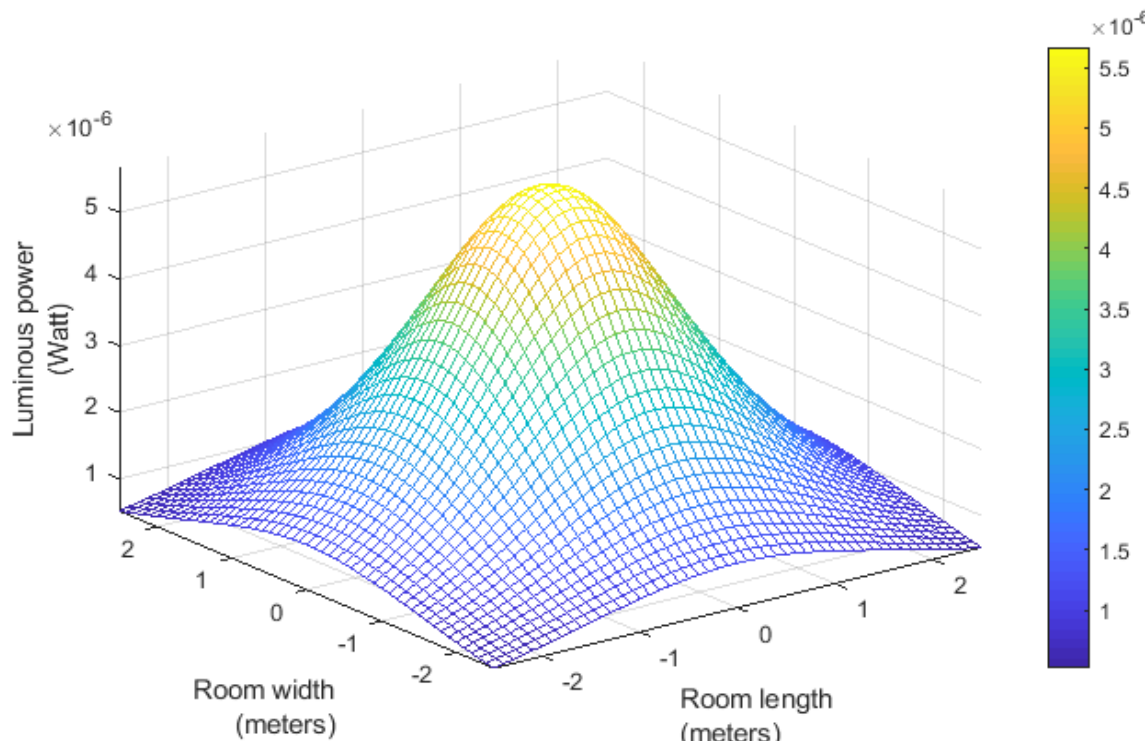


Figure 5.1: Received power 20mw

As a result, the advantage of these simulations is to build a good coverage plane for Li-Fi APs in a typical area.

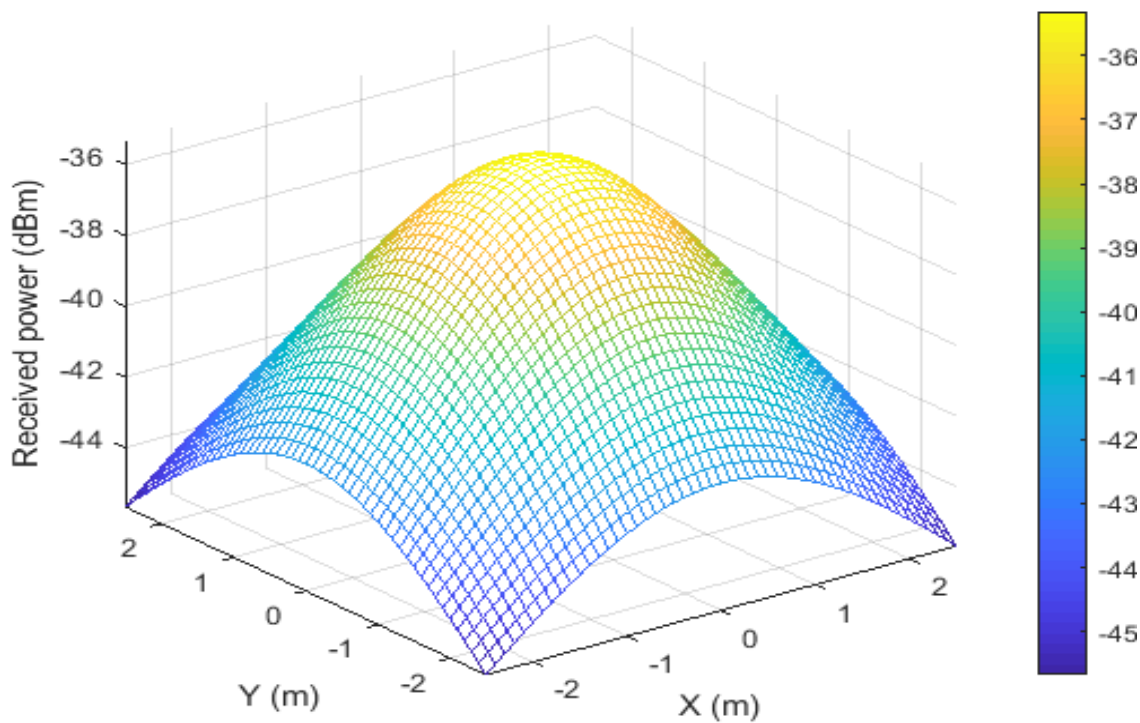


Figure 5.2: The optical channel gain

5.3 Modulation type versus BER:

In this section, we calculate the BER for modulations OOK and L-PPM. By calculating some equations and calling BER function to give results when sending a signal. In this simulation, we used an optical channel for the communicated signal calculation results of the communicated signal, which was produced randomly and matched in the receiver. The process in this simulation is to reduce errors that might have occurred during the transmission time.

5.3.1 Bit Error Rate and E_b/N_0 for OOK :

An analysis of the BER as a function of SNR, with theoretical and simulation results in Fig. 5.3. The range of x-axes for the SNR, the BER begins to decrease as the SNR values begin to increase. The results given to BER equations are AWGN because of ambient light in Fig. 5.4.

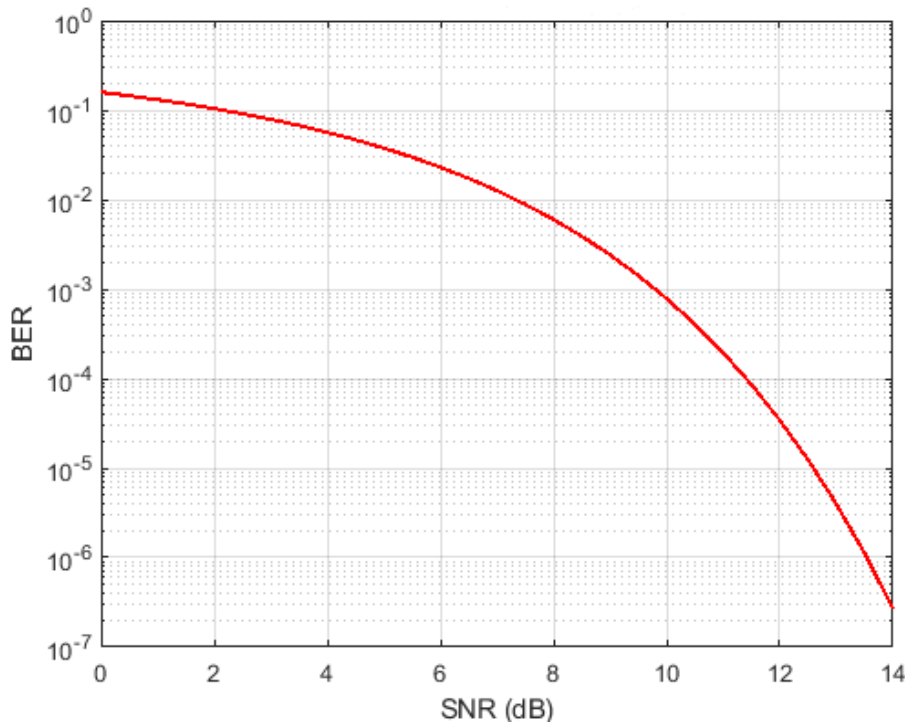


Figure 5.3: Bit error curve for OOK modulation ,using power 20mw

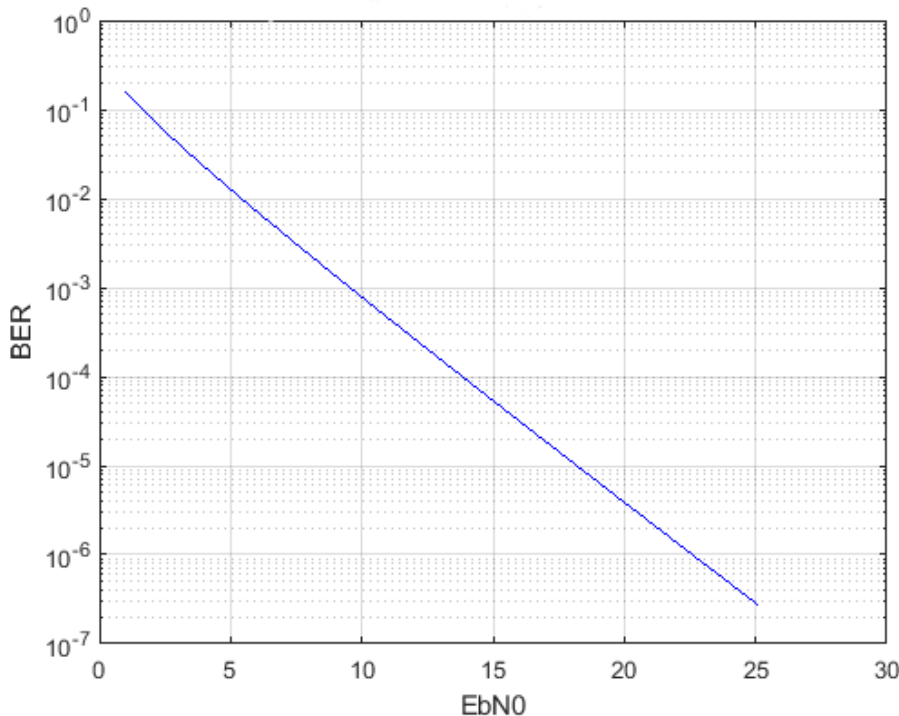


Figure 5.4: BER to E_b/N_0 for OOK modulation, using power 20mw

The range of x-axes for the E_b/N_o , and the range of y-axes for the BER begins to decrease as the E_b/N_o values begin to increase Semi-linear. These are the results using the power is 20mw.

Changed the power at 10 mw, see how this would affect the results, this can be explained in the BER to SNR analysis result in the Fig. 5.5, and in Fig. 5.6 BER to E_b/N_0 Also using changing the power to 10 mw.

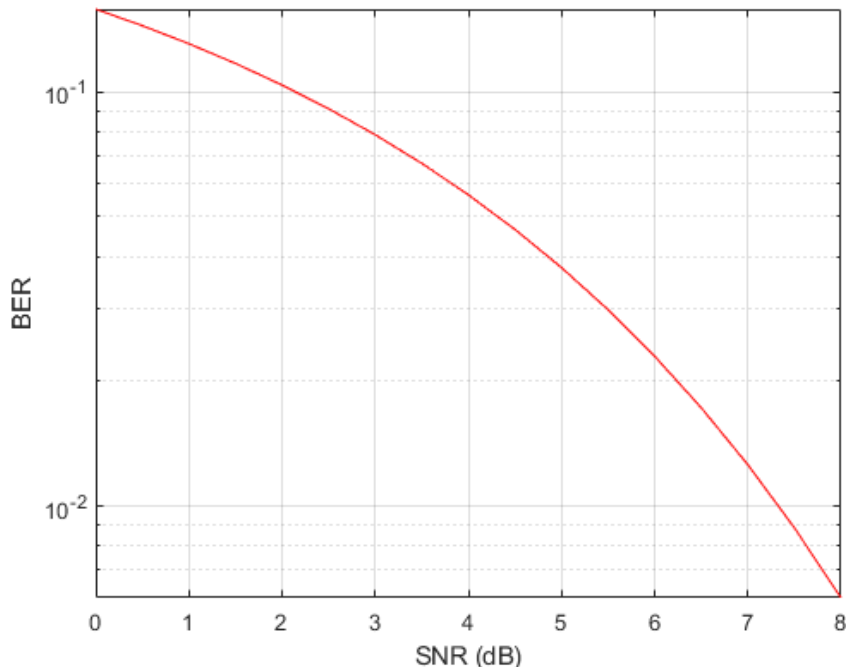


Figure 5.5: Bit error curve for OOK modulation , (power 10 mw)

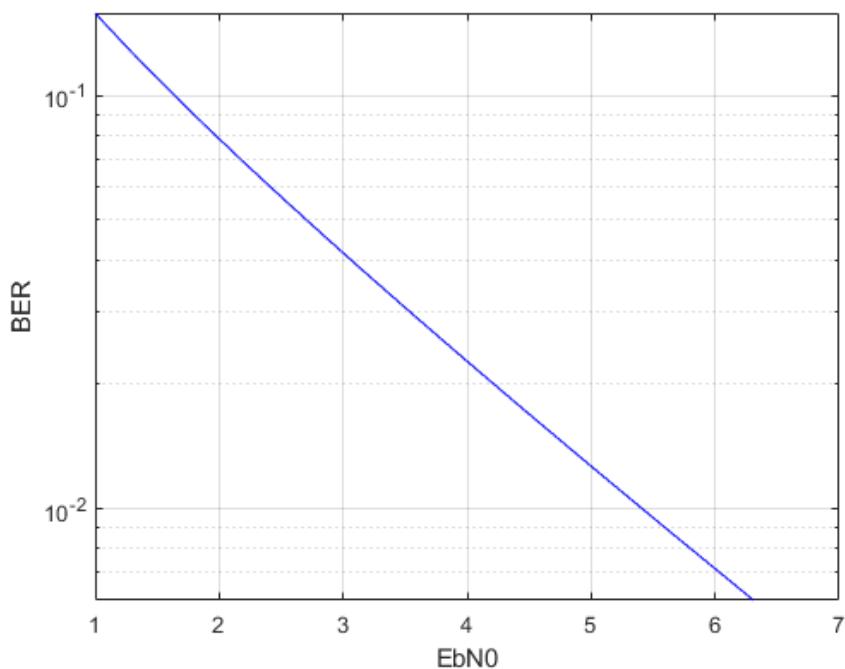


Figure 5.6: BER to E_b/N_0 for OOK modulation, (power 10 mw)

Observe that there is a change in BER and SNR using the power value is changed.

5.3.2 Bit Error Rate/Slot Error Rate of L-PPM :

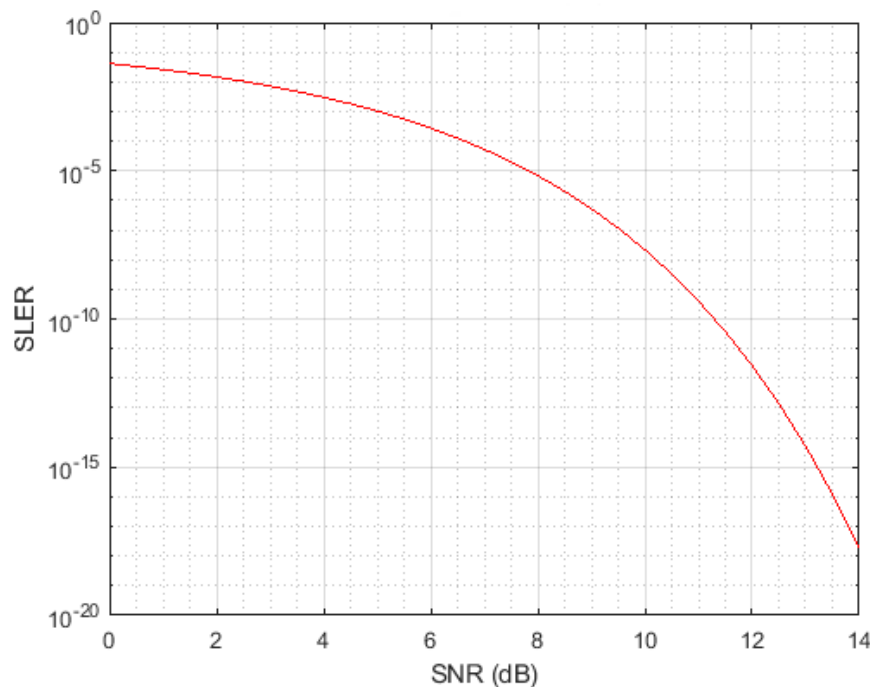


Figure 5.7: Bit error rate curve for 8-PPM modulation ,(power 20 mw)

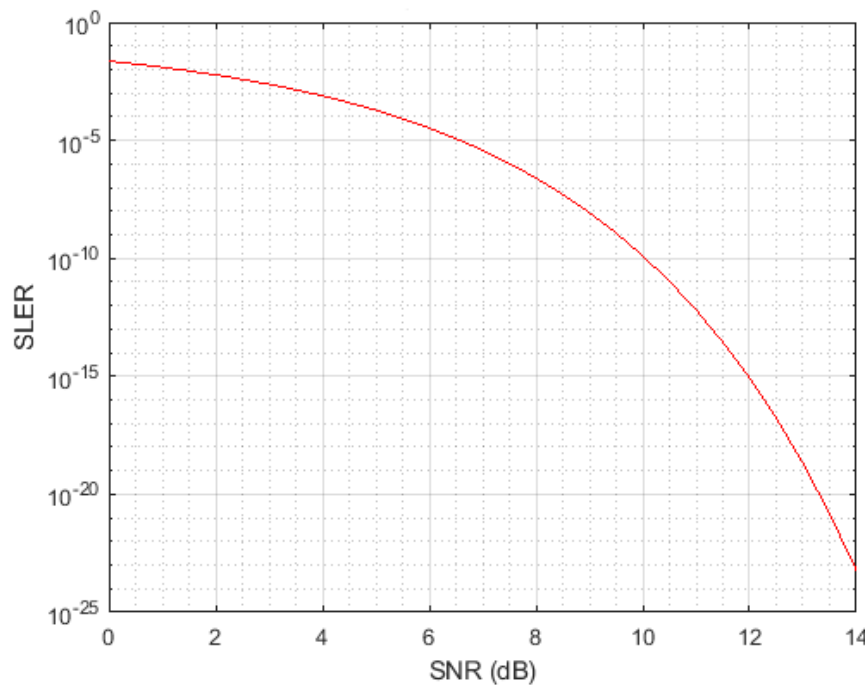


Figure 5.8: Bit error rate curve for 16-PPM modulation , (power 20 mw)

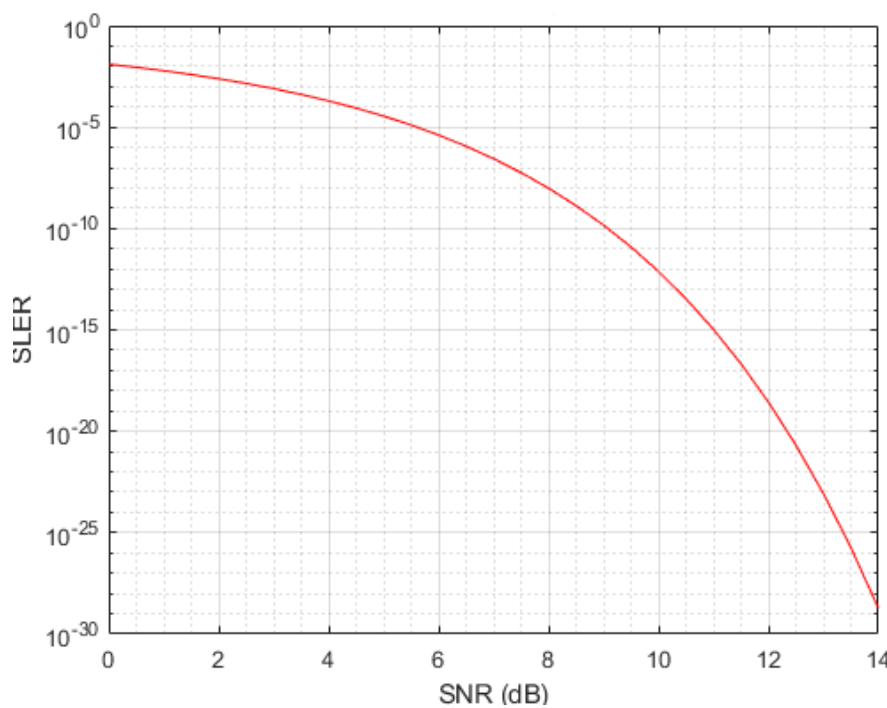


Figure 5.9: Bit error rate curve for 32-PPM modulation, (power 20 mw)

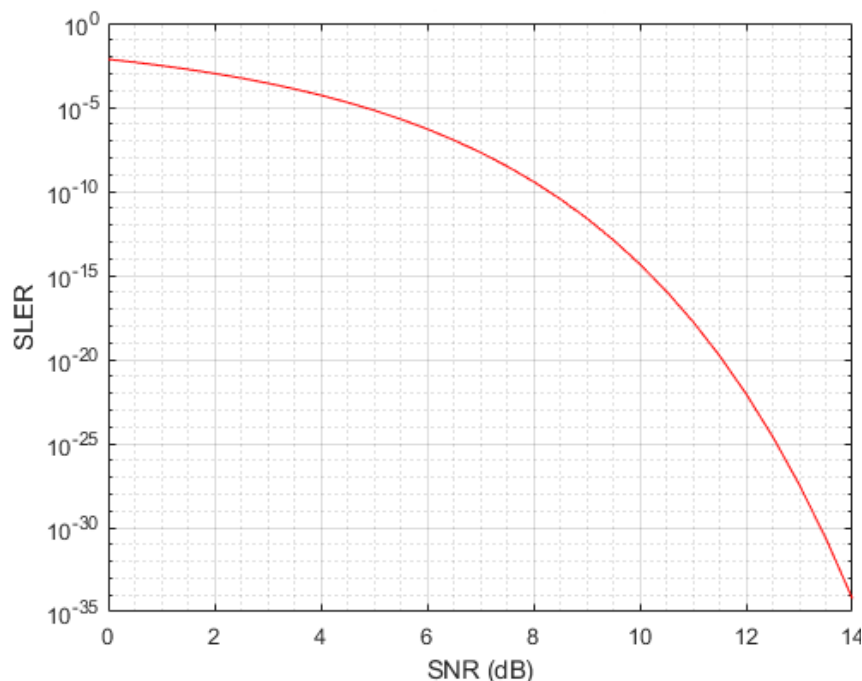


Figure 5.10: Bit error rate curve for 64-PPM modulation , (power 20 mw)

The analysis of the Slot Error Rate (SLER) as a function of SNR with theoretical and simulation results in Fig. 5.7 , 5.8 , 5.9, and 5.10.

The range of x-axes for the SNR, the SLER begins to decrease as the SNR values begin to

increase. These are the results using the power is 20 mw.

Changed the power at 10 mw, see how this would affect the results , this can be explained in the SLER to SNR analysis result in the Fig. 5.13, 5.14, 5.24, and 5.11.

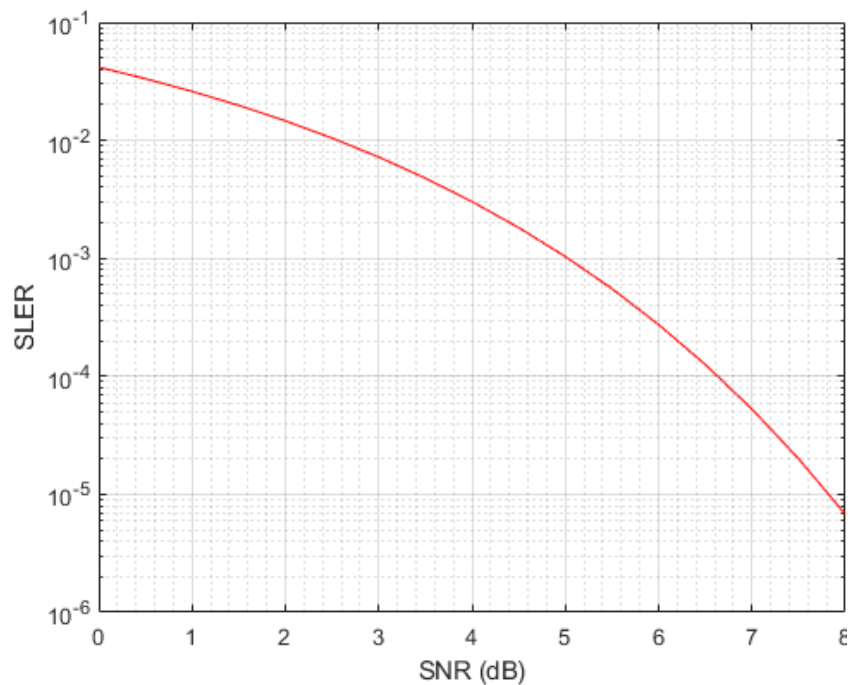


Figure 5.11: Bit error rate curve for 8-PPM modulation, (power 10 mw)

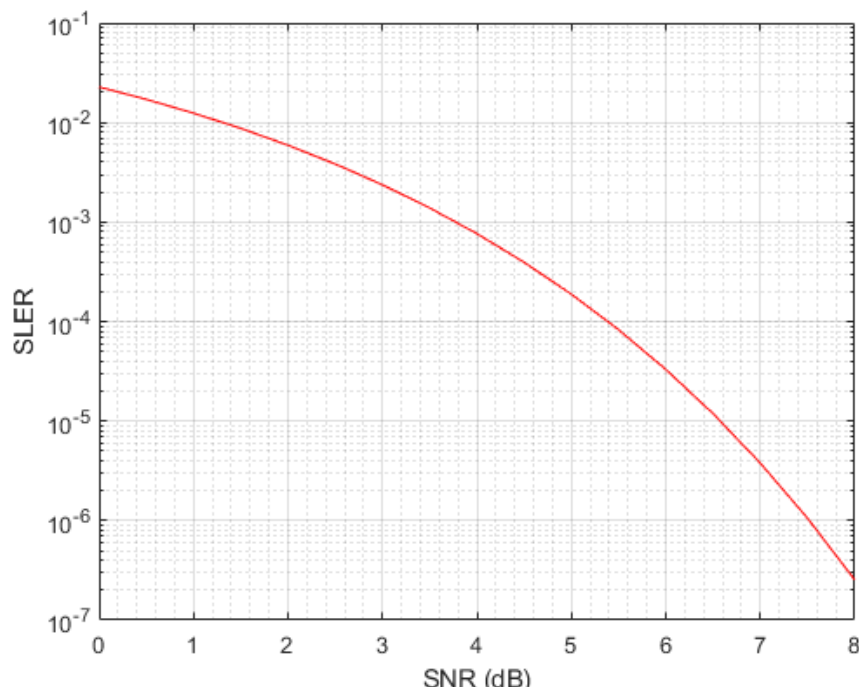


Figure 5.12: Bit error rate curve for 16-PPM modulation, (power 10 mw)

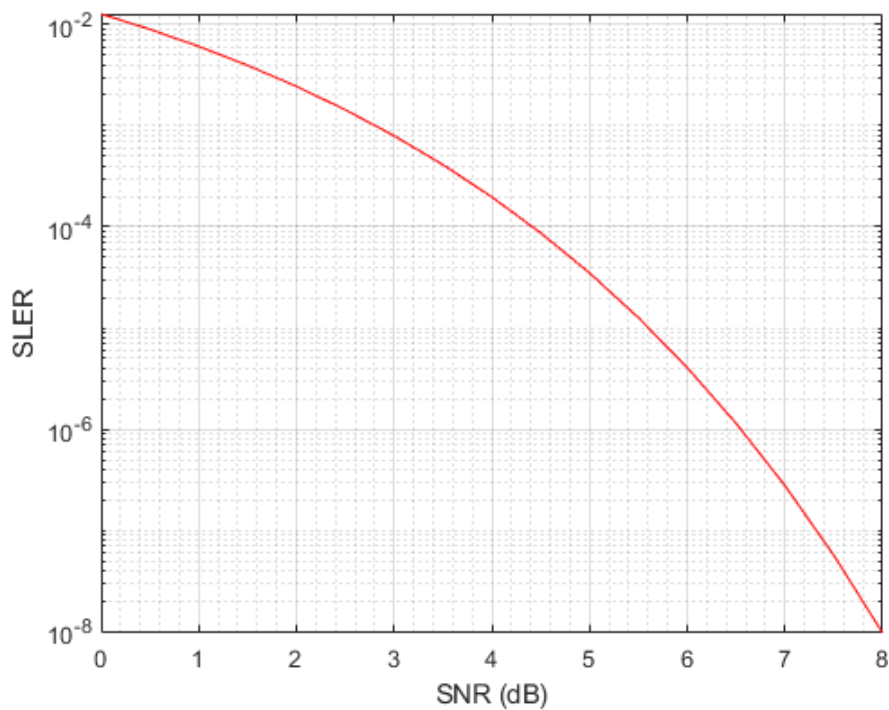


Figure 5.13: Bit error rate curve for 32-PPM modulation , (power 10 mw)

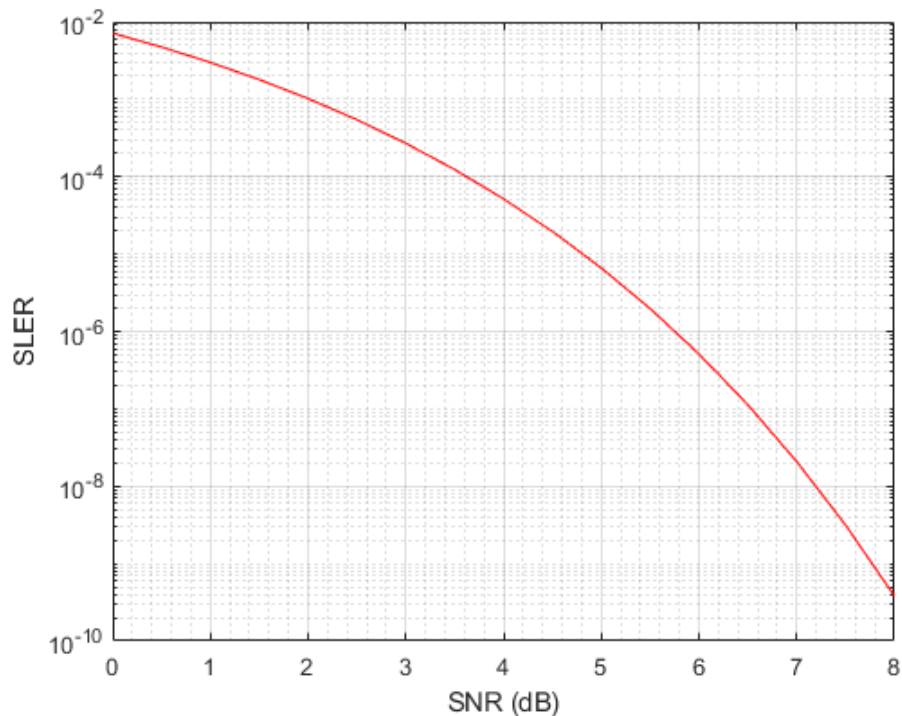


Figure 5.14: Bit error rate curve for 64-PPM modulation , (power 10 mw)

Observe that there is a change in the SLER, and the SNR using the power value is changed.

5.3.3 Comparison Between Different PPM and OOK Schemes

In this section, we compare the results obtained from the previous section.

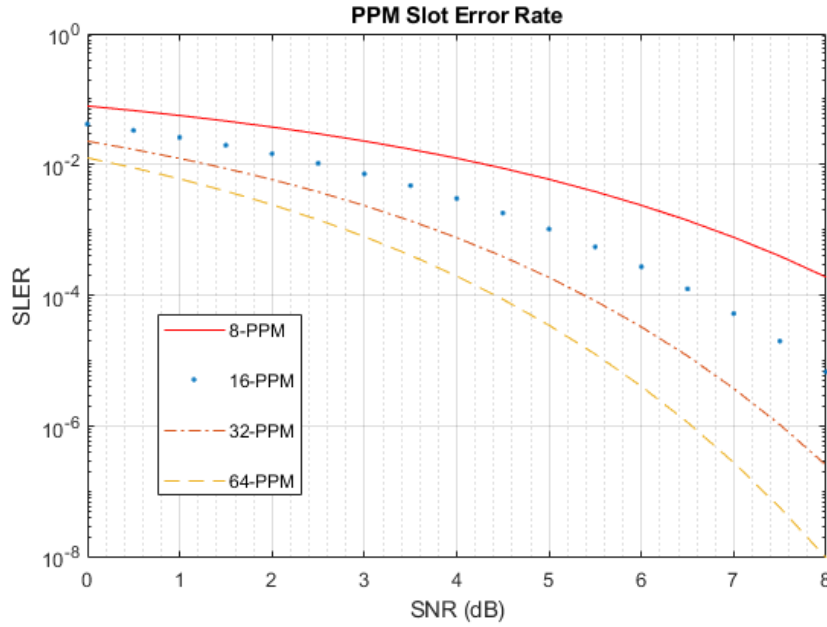


Figure 5.15: Slot error rate curve for L-PPM modulation, (power 10 mw)

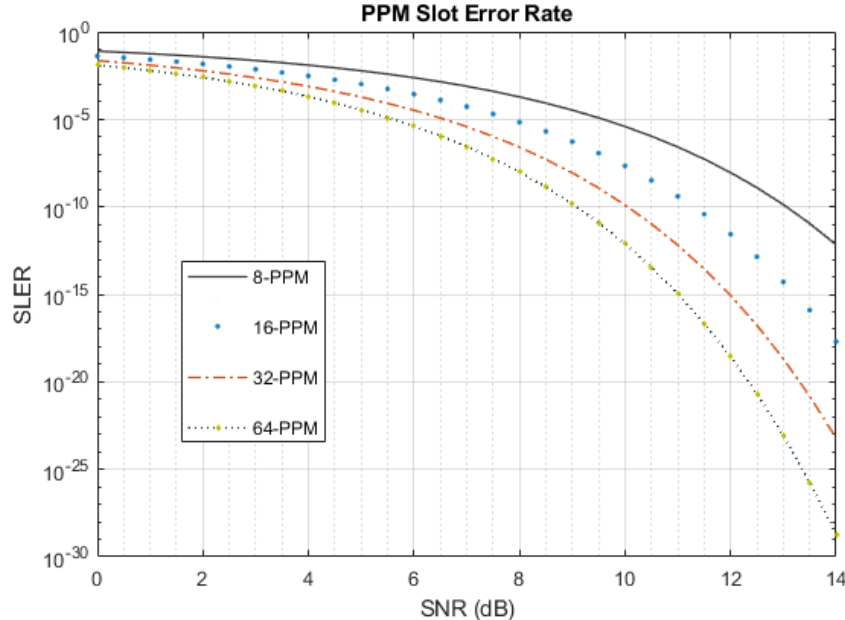


Figure 5.16: Slot error rate curve for L-PPM modulation, (power 20 mw)

In Fig. 5.15, the results show different L-PPM, using the power 10 mw. and this Fig. 5.16, the results using the power 20 mw.

After a comparison when sending a random-signal using L- PPM modulation, when changing

the value of L-PPM , SLER was changing but SNR not changing, that is,

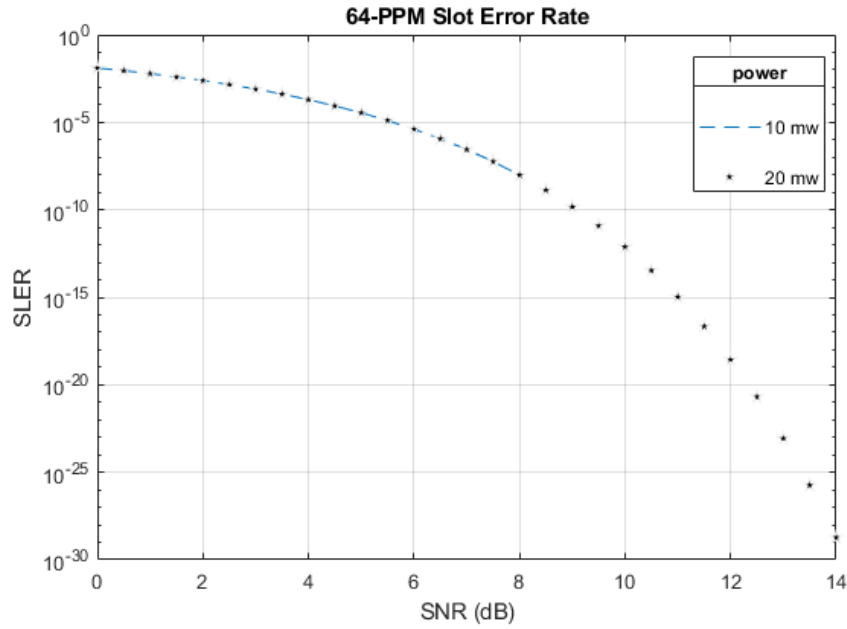


Figure 5.17: Difference between power in SLER for 64-PPM modulation

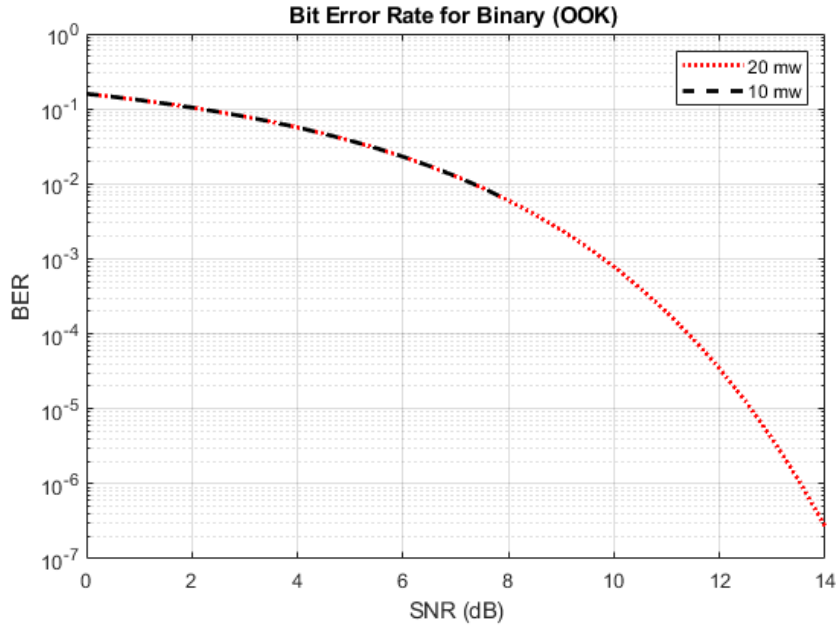


Figure 5.18: Difference between power in BER for OOK modulation

we notice through results in the figure that 64-PPM is best. Based on this results, the SLER is affected in PPM when the number of bit is changed.

A difference using changing the power in 64-PPM and OOK, in Fig. 5.17, 5.18.

It shows that when the power is increased, give rise to an increase in the SNR and a decrease in the SLER/ BER. Based on these results, a power effects of the SNR and SLER/BER in the

modulations OOK and L-PPM.

5.4 Image transmission using QAM and QPSK modulation:

This section shows the results of simulated image transmission using two different modulations: QPSK and QAM.

The pre-modulation original image is illustrated in Fig. 5.19.

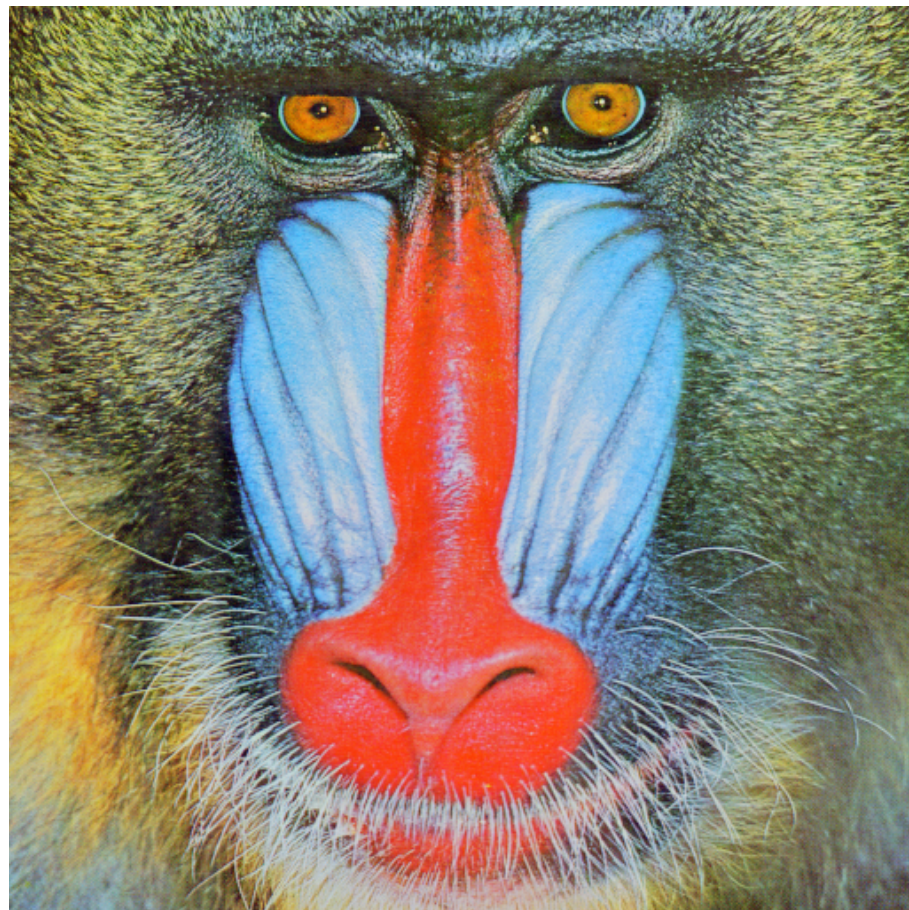


Figure 5.19: Original image before transmission

And in Fig. 5.20 and 5.21, after a process of modulation with 16-QAM and 64-QAM. this results using the power is 20 mw.

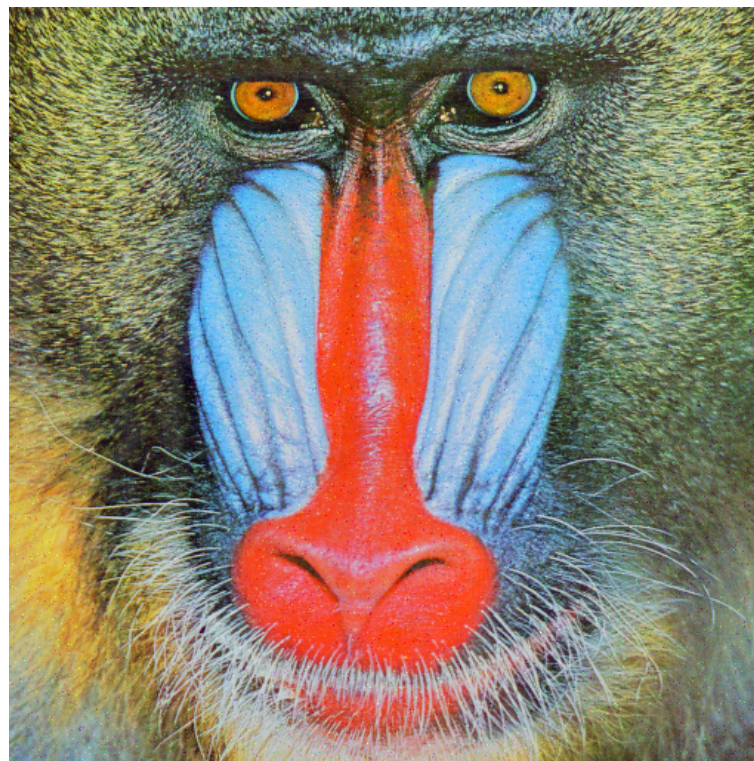


Figure 5.20: Transmission the image using 16-QAM modulation, (power 20 mw)

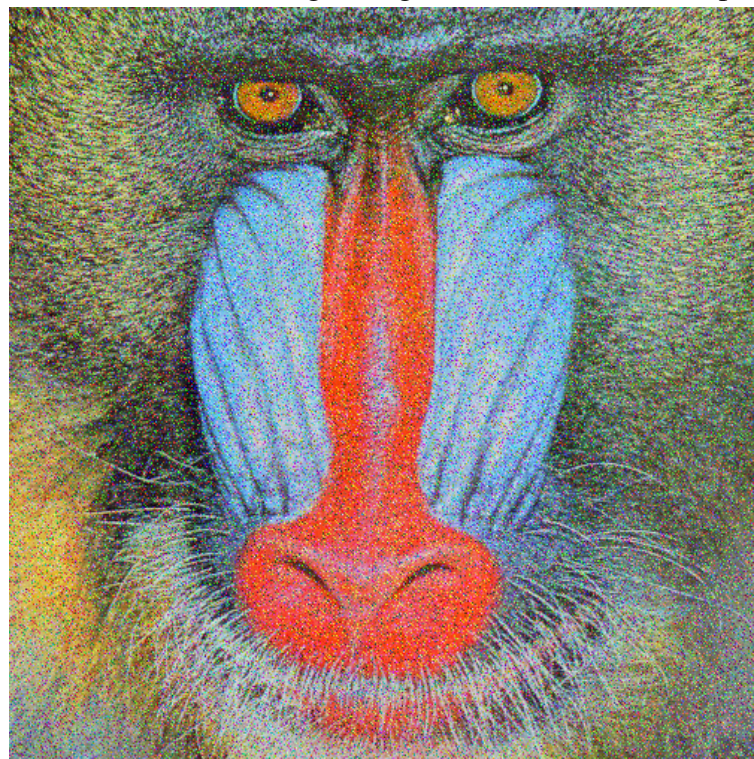


Figure 5.21: Transmission the image using 64-QAM modulation, (power 20 mw)

And in Fig. 5.22, explain the image after a process of modulation 16-QPSK.

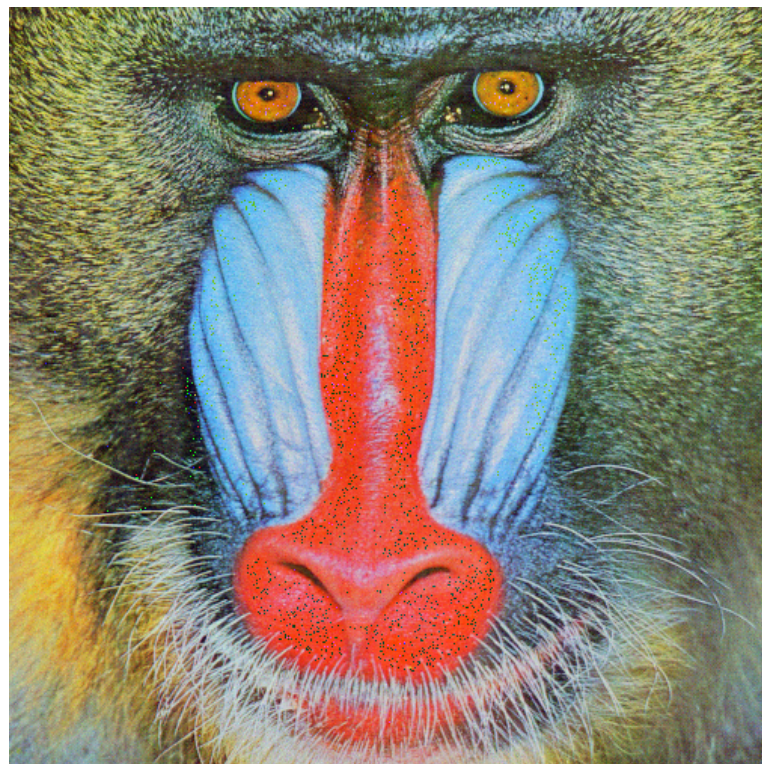


Figure 5.22: Transmission the image using 16-QPSK modulation, (power 20 mw)

The image error resulting from the modulation was calculated by MSE as described in the previous chapter 4 of this section (4.6.2). this can be explained in Fig. 5.23.

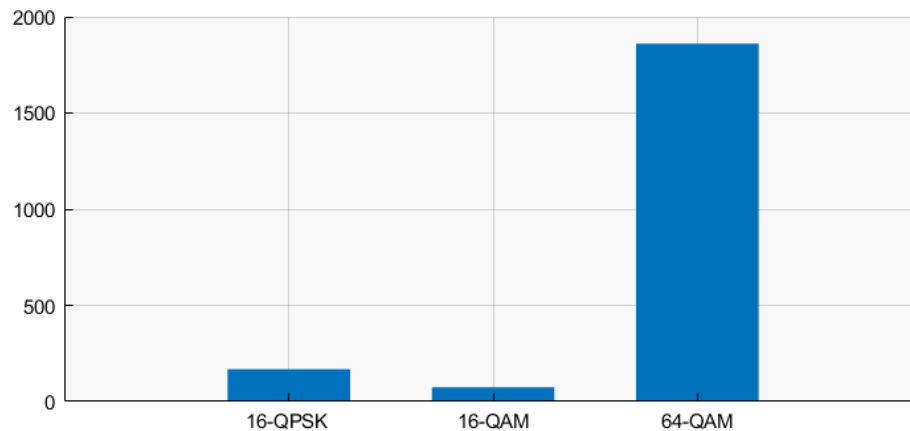


Figure 5.23: Mean Squared Error (Power 20 mw)

Changed the power at 10 mw, see how this would affect the results, as shown in the Fig. 5.24 when the modulation 16-QAM. And in Fig 5.25 when the modulation 64-QAM.

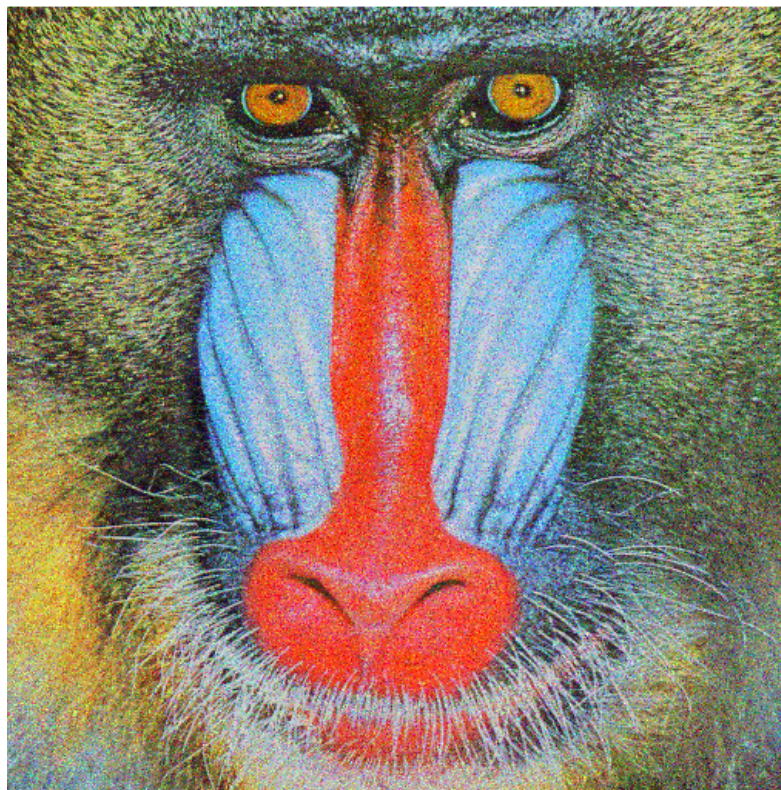


Figure 5.24: transmission the image using 16-QAM modulation, (power 10 mw)

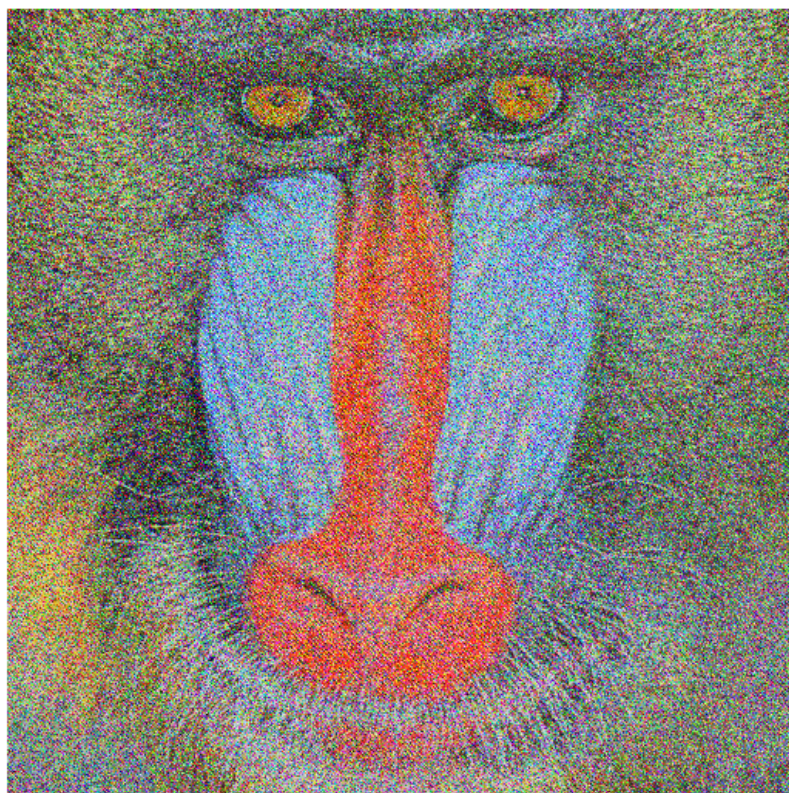


Figure 5.25: transmission the image using 64-QAM modulation, (power 10 mw)

And in Fig. 5.26, explain the image after a process of modulation 16-QPSK.

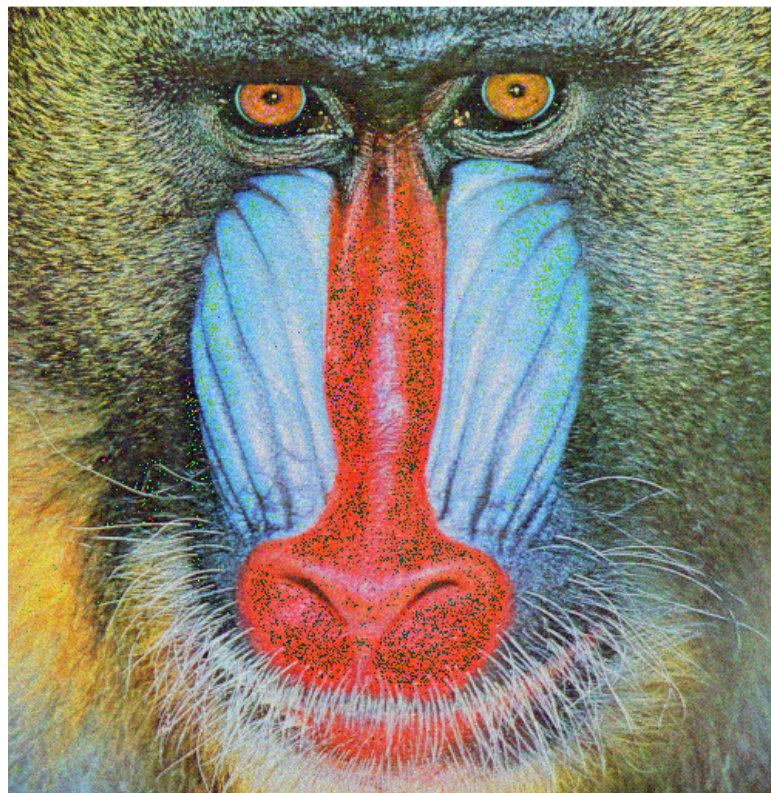


Figure 5.26: transmission the image using 16-QPSK modulation, (power 10 mw)

As shown in the Fig. 5.27, the image error resulting from the modulation after changing the power.

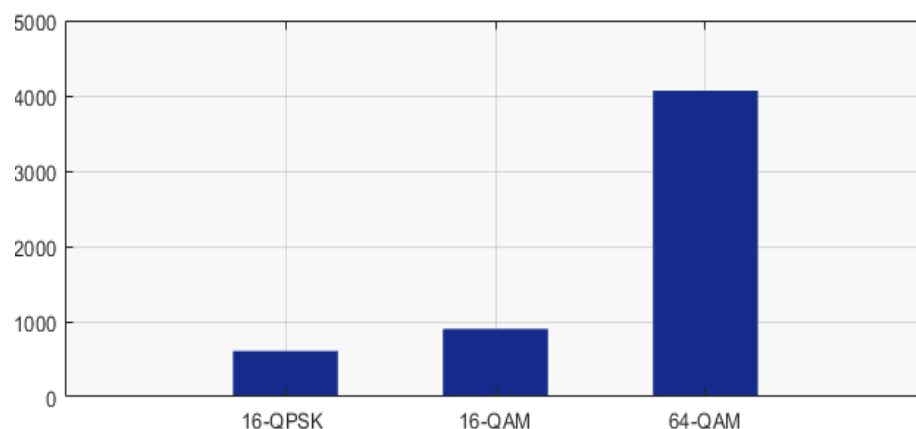


Figure 5.27: Mean Squared Error, (power 10 mw)

Observe that there is a change in the MSE when the power value is changed. In this section, we explained the results when sending images, then calculating the MSE, and changing the

power, we noticed that the power affects the noise, as shown in Fig 5.27.

When comparing the results, we find that the QPSK modulation is affected by the power change less than the effect of 16-QAM and 64-QAM, as shown in the Fig. 5.23 as using the power 20mw and the Fig. 5.27 the power 10mw.

5.5 Summary

In this chapter, after testing all components of the proposed system and get good results the whole proposed LIFI system has been implemented, and We simulated the LOS channel and used modulations: OOK, PPM, QAM, and QPSK. we used the QAM And QPSK to transmission Photo, estimate the BER, and its representation using curves.

Chapter 6

Conclusion and Future Work

6.1 Conclusion

In this project, we discussed a Li-Fi system to simulation this system through our study, We've explained all the blocks in the system, the most important blocks were: the transmitter, the receiver, the channel, and also the modulation.

We also studied the modulation, and most commonly used types of modulation are OOK and PPM. after the study we've carried out a simulation of the LOS channel in an empty room, and the distribution of energy in the room, and we calculated the BER when sending a random signal and used two different values of the power, we've noticed a difference in the BER between modulation after changed the power, and also observed at calculated the BER a difference between OOK and PPM, thus we concluded from this that when the power was less, when the BER was greater.

Thereafter, We sent an image using two other types of modulation QAM and QPSK, we also used two values of power, first we sent an image in 16-QAM, 64-QAM, and 64-QPSK modulations, and calculated the image quality using MSE, Through MSE calculation of the image, the error in the 16-QAM modulation transmitted image, we less than the 64-QAM and QPSK.

When increasing the power and sending the image with the same previous modulation types, the computation of quality error was less when the power was greater. That is, We conclude that the higher the power is greater, the error less at the MSE calculation.

And also, we conclude that the effect of the QPSK modulation when changing the power was less than QAM. This indicates that when calculating MSE, the QPSK modulation was less than 16-QAM and 64-QAM.

6.2 Future Work

- Implementation of video transmission over Li-Fi using physical devices.
- increased spectrum efficiency Using hybrid VLC/RF network.
- use OFDM for transmitting at high data rates and high spectral efficiency.

Bibliography

- [1] L. I. Albraheem, L. H. Alhudaithy, A. A. Aljaser, M. R. Aldhafian, and G. M. Bahliwah, “Toward designing a li-fi-based hierarchical iot architecture,” *IEEE Access*, vol. 6, pp. 40 811–40 825, 2018.
- [2] Y. Wang, X. Wu, and H. Haas, “Fuzzy logic based dynamic handover scheme for indoor li-fi and rf hybrid network,” in *2016 IEEE International Conference on Communications (ICC)*, 2016, pp. 1–6.
- [3] L. U. Khan, “Visible light communication: Applications, architecture, standardization and research challenges,” *Digital Communications and Networks*, vol. 3, no. 2, pp. 78 – 88, 2017. [Online]. Available: <http://www.sciencedirect.com/science/article/pii/S2352864816300335>
- [4] A. R. Ndjongue, T. M. Ngatched, O. A. Dobre, and A. G. Armada, “Vlc-based networking: Feasibility and challenges,” *IEEE Network*, 2020.
- [5] A. Jovicic, J. Li, and T. Richardson, “Visible light communication: opportunities, challenges and the path to market,” *IEEE Communications Magazine*, vol. 51, no. 12, pp. 26–32, 2013.
- [6] R. Sagotra and R. Aggarwal, “Visible light communication,” *International Journal of Computer Trends and Technology (IJCTT) volume4 Issue4*, pp. 906–910, 2013.
- [7] H. Haas, “Lifi: Conceptions, misconceptions and opportunities,” in *2016 IEEE Photonics Conference (IPC)*, 2016, pp. 680–681.
- [8] L. I. Albraheem, L. H. Alhudaithy, A. A. Aljaser, M. R. Aldhafian, and G. M. Bahliwah, “Toward designing a li-fi-based hierarchical iot architecture,” *IEEE Access*, vol. 6, pp. 40 811–40 825, 2018.

- [9] H. Alshaer and H. Haas, “Bidirectional lifi attocell access point slicing scheme,” *IEEE Transactions on Network and Service Management*, vol. 15, no. 3, pp. 909–922, 2018.
- [10] S. Naribole, S. Chen, E. Heng, and E. Knightly, “Lira: A wlan architecture for visible light communication with a wi-fi uplink,” in *2017 14th Annual IEEE International Conference on Sensing, Communication, and Networking (SECON)*, 2017, pp. 1–9.
- [11] H. Elgala, R. Mesleh, H. Haas, and B. Pricope, “Ofdm visible light wireless communication based on white leds,” in *2007 IEEE 65th Vehicular Technology Conference - VTC2007-Spring*, 2007, pp. 2185–2189.
- [12] Z. Ghassemlooy, W. Popoola, and S. Rajbhandari, *Optical Wireless Communications: System and Channel Modelling with MATLAB*, 1st ed. USA: CRC Press, Inc., 2012.
- [13] J. Rufo, J. Rabadan, F. Delgado, C. Quintana, and R. Perez-Jimenez, “Experimental evaluation of video transmission through led illumination devices,” *IEEE Transactions on Consumer Electronics*, vol. 56, no. 3, pp. 1411–1416, 2010.
- [14] O. Narmanlioglu, B. Turan, B. Kebapci, S. C. Ergen, and M. Uysal, “Poster: On-board camera video transmission over vehicular vlc,” in *2016 IEEE Vehicular Networking Conference (VNC)*, 2016, pp. 1–2.
- [15] M. B. Rahaim, A. M. Vegni, and T. D. C. Little, “A hybrid radio frequency and broadcast visible light communication system,” in *2011 IEEE GLOBECOM Workshops (GC Wkshps)*, 2011, pp. 792–796.
- [16] S. Shao, A. Khreichah, M. Ayyash, M. B. Rahaim, H. Elgala, V. Jungnickel, D. Schulz, T. D. C. Little, J. Hilt, and R. Freund, “Design and analysis of a visible-light-communication enhanced wifi system,” *IEEE/OSA Journal of Optical Communications and Networking*, vol. 7, no. 10, pp. 960–973, 2015.
- [17] M. S. Islim and H. Haas, “Modulation techniques for li-fi,” *ZTE communications*, vol. 14, pp. 29–40, 2016.
- [18] H. W. Moazzam, U. Ayub, A. Shahzad, and M. Shahid, “Design and implementation of visible light communication using error correcting turbo codes,” 2018.

- [19] X. Bao, G. Yu, J. Dai, and X. Zhu, “Li-fi: Light fidelity-a survey,” *Wireless Networks*, vol. 21, pp. 1879–1889, 2015.
- [20] M. Z. Afgani, H. Haas, H. Elgala, and D. Knipp, “Visible light communication using ofdm,” in *2nd International Conference on Testbeds and Research Infrastructures for the Development of Networks and Communities, 2006. TRIDENTCOM 2006.*, 2006, pp. 6 pp.–134.
- [21] J. Jiang, Y. Huo, F. Jin, P. Zhang, Z. Wang, Z. Xu, H. Haas, and L. Hanzo, “Video streaming in the multiuser indoor visible light downlink,” *IEEE Access*, vol. 3, pp. 2959–2986, 2015.
- [22] D. K. Son, E. B. Cho, and C. G. Lee, “Demonstration of visible light communication link for audio and video transmission,” in *2010 Photonics Global Conference*, 2010, pp. 1–4.
- [23] K. P. Pujapanda, “Lifi integrated to power-lines for smart illumination cum communication,” in *2013 International Conference on Communication Systems and Network Technologies*, 2013, pp. 875–878.
- [24] H. Haas and C. Chen, “What is lifi?” in *2015 European Conference on Optical Communication (ECOC)*, 2015, pp. 1–3.
- [25] N. Chi, “Led-based visible light communications,” in *2018 Springer Verlag Berlin Heidelberg*, 2018, pp. 1–245.
- [26] X. Li, “Simulink-based simulation of quadrature amplitude modulation (qam) system,” in *Proceedings of the 2008 IAJC-IJME International Conference*, 2008.
- [27] T. D. Memon, W. Ghangro, B. S. Chowdhry, and A. A. shaikh, “Quadrature phase shift keying modulator demodulator for wireless modem,” in *2009 2nd International Conference on Computer, Control and Communication*, 2009, pp. 1–6.
- [28] U. Sara, M. Akter, and M. S. Uddin, “Image quality assessment through fsim, ssim, mse and psnr—a comparative study,” *Journal of Computational Chemistry*, vol. 7, pp. 8–18, 2019.

Appendix A (Li-Fi):

```

theta=70
% semi-angle at half power
m=-log10(2)/log10(cosd(theta));
%Lambertian order of emission
P_total=20;
%transmitted optical power by individual LED
Adet=1e-4;
%detector physical area of a PD
Ts=1 ;
%gain of an optical filter; ignore if no filter is used
index=1.5;
%refractive index of a lens at a PD; ignore if no lens is used
FOV=60*pi/180; %FOV of a receiver
G_Con=(index^2)/sin(FOV);
%gain of an optical concentrator;
%ignore if no lens is used
lx=5; ly=5; lz=3;% room dimension in metre
h=2.15;
%the distance between source and receiver plane
XT=0; YT=0           % position of LED;
Nx=lx*10; Ny=ly*10;
% number of grid in the receiver plane
x=-lx/2:lx/Nx:lx/2;
y=-ly/2:ly/Ny:ly/2;
[XR,YR]=meshgrid(x,y);      % receiver plane grid
D1=sqrt((XR-XT(1,1)).^2+(YR-YT(1,1)).^2+h.^2);
% distance vector from source 1
cosphi_A1=h./D1; % angle vector
H_A1=(m+1)*Adet.*cosphi_A1.^ (m+1)./(2*pi.*D1.^2);
% channel DC gain for source 1

```

```

P_rec=P_total.*H_A1.*Ts.*G_Con;      % received power
P_rec_dBm=10*log10(P_rec);

%% Line of site Channel Gain
meshc(x,y,P_rec_dBm);
xlabel('X (m)');
ylabel('Y (m)');
zlabel('Received power (dBm)');
axis([-lx/2 lx/2 -ly/2 ly/2 min(min(P_rec_dBm)) max(max(P_rec_dBm))]);
title('Line of site Channel Gain');

%% Received Power
figure(2)
meshc(x,y,H_A1);
xlabel({'Room length', '(meters')});
ylabel ({'Room width', '(meters')});
zlabel ({'Luminous power', '(Watt')});
axis([-lx/2 lx/2 -ly/2 ly/2 min(min(H_A1)) max(max(H_A1))]);
title({'Received Power'});

Dr= 115200;          %Data rate
Iamb = 7E-8;         % Ambient light power (Ampere) %
q = 1.60E-19;        % Electron charge (C)
Ba = 4.5E6;          % Amplifier bandwidth (Hz) %
Iamf = 5e-12 ;
% Amplifier noise density (Ampere/Hz^0.5)%
R_rx = 0.6;          %responsivity of receiver
D=1.48 ;             %distance between Tx & Rx

%% Line of sight (los )
M=-log(2)/log(cos(theta)) ;
% Order of Lambertian emission

```

```

Ro= ((M+1) / (2*pi)) * cos(theta)^M ;
% Lambertian radiant intensity

H_Los = (ar./D.^2).*cos(phi)*Ro ; %Channel transfer function

Prx_los = P_led * H_Los ; % Rx power of los

%% call function Noise
[T_noise] = Noise ( Dr,q,R_rx,Iamf,Prx_los,Ba);

%% Signal to noise ratio (SNR)
SNR = (R_rx *Prx_los).^2 / T_noise ;
SNR_db = 10* log10 (SNR);

%% puls pustion modulation parametar
Bo=5 ; %Bit order
Lsy=2^Bo; %symbol length
nsym=200; %number of PPM symbols
Lsig=nsym*Lsy; %total length of PPM slots
Rsymb=1e6; %slot rate symbol rate
Rb=(Rsymb*Bo); %Bit rate
Tb =1/Rb ;

%%
SNRdb= 0:0.5:SNR_db; %Energy per bit db
EsN0=SNRdb+10*log10(Bo); %Energy per symbol db
SNR_e= 10.^ (SNRdb./10); %Energy per bit Eb/N0
EbN0=10.^ (SNRdb./10);

%% Call Function PPM Modulation
PPM=ppm(Bo,nsym);
%function to generate PPM signal 0
PPM = PPM*1;
%Matlab logic signal in double
for i=1:length(SNRdb)

Pavg(i) =(1/Lsy)*sqrt(((2*Bo)*T_noise*Rsymb*SNR_e(i)) / (2*R_rx.^2)); %Lum

```

```

Ipeak(i) = Lsy*R_rx*Pavg(i); %Photodiode Current
Epeak(i) = Lsy*Bo*Ipeak(i)^2 * Tb; %Peak current energy
sigma(i)=sqrt(T_noise*Epeak(i)/(2)); %standard deviation after receiver
threshold=0.5*Epeak(i); %threshold level
for j=1 : Lsig
MF_out(j) = PPM(j)*Epeak(i)+ normrnd(0,sigma(i));
%matched filter output
end
received_PPM=zeros(1,Lsig);
%generating empty PPM vector
received_PPM(find(MF_out> threshold))=1;
%generating the received signal
[No_of_Error(i) ser_hdd(i)]= biterr(received_PPM,PPM);
%Matlab function to calculate the SER
end
%%

figure(1)
semilogy(SNRdb ,ser_hdd,'magenta'); %simulation BER graph
ylabel('SLER'); xlabel('SNR (dB)');
title([num2str(Lsy), '-PPM SlotErrorRate']);
grid on
grid minor
hold on;
%% theoretical calculation
Pse_ppm_theor=qfunc(sqrt(Bo*SNR_e));
%transform SLER to SER
semilogy(SNRdb ,Pse_ppm_theor,'red','linewidth',0.5); %theoretical BER

```

```

%% Call function to OOK Modulation

[theorBER,simuBER] = OOK(SNRdb,Rb,SNR_e,R_rx,T_noise);

figure(2)

semilogy(SNRdb,theorBER,'red'); %theoretical BER graph
grid on
ylabel('BER');
xlabel('SNR (dB)');
title('Bit Error Rate for Binary (OOK) ');
hold on

%% theoretical BER and Eb/N0 graph

figure(4)

semilogy(EbN0,theorBER,'blue');
grid on
ylabel('BER');
xlabel('EbN0');
title('Bit Error probability curve for Binary (OOK) ');
hold on

%% Call Function Qam & QPSK Modulation

[im_qpsk,im_16qam,im_64qam,in] = QAM_and_Qpsk(SNRdb);

figure(6);
imshow(im_qpsk);
title('QPSK');

figure(7);
imshow(im_16qam);
title('16QAM');

figure(8);
imshow(im_64qam);title('64QAM');

%% MSE Mean-squared error

s=immse(im_qpsk,in);
s16=immse(im_16qam,in);

```

```
s64=immse(im_64qam,in)'

y=[s s16 s64];
x=1:3 ;
figure;
bar(x,y,'blue');
title(" Mean squared error");
set(gca,'xticklabel',{"16-QPSK" "16-QAM" , "64-QAM"})
```

Apindex B (Noise) :

```
function [T_noise] = Noise( Dr , q , R_rx , Iamf , Prx_los , Ba)
 $\% \text{ Calculate Noise in System}$ 
I2=0.562 ;  $\% \text{noise bandwdith factor}$ 
Bn= I2 *Dr ;  $\% \text{Noise Bandwidth}$ 
P_amb = Iamf / R_rx ;
P_total= Prx_los * P_amb ;
shot_n = 2*q * R_rx * P_total * Bn ;  $\% \text{ shot noise}$ 
Amp_n = Iamf^2 * Ba ;  $\% \text{ Amplifier noise variance}$ 
T_noise = Amp_n + shot_n;  $\% \text{ Total noise}$ 
end
```

Appendix C (Function to PPM)

```
function PPM=ppm (Bo,nsym)
 $\% \text{ function to PPM}$ 
 $\% \text{'Bo' bit order}$ 
 $\% \text{'nsym': number of PPM symbol to generate}$ 
PPM=[];  $\% \text{PPM array empty inizialization}$ 
for i= 1:nsym
 $\% \text{cycle from 1 to number of symbol,every cycle generate one symbol}$ 
bitSig= rand (1,Bo)> 0.5;  $\% \text{ random binary number}$ 
dec_value=bi2de(bitSig,'left-msb');  $\% \text{converting bit to decimal value}$ 
tempPPM=zeros(1,2^Bo);  $\% \text{zero sequence of length } 2^M$ 
```

```

tempPPM(dec_value+1)=1;
%placing a pulse according to decimal value,
%matlab index start from 1 and not from 0, so need to add 1;
PPM=[PPM tempPPM];           %put tempPPM in array queue
end                         %close for cycle
end

```

Appendix D (Function to OOK)

```

function [theorBER ,simuBER ] = OOK(SNRdb,Rb,SNR_e,R_rx,T_noise)
%OOK Summary of this function goes here
nSignal=1000;
Tbit=1/Rb;
randombinary = rand (1,nSignal)> 0.5; % Random Binary Signal
randombinary = randombinary *1; %transform logical input in double
for i=1:length(SNRdb)           %SNR_db cycle
Pavg(i) = sqrt ((T_noise*Rb*SNR_e(i))/(2*R_rx^2)); %Luminous power
Ipeak(i) = 2*R_rx*Pavg(i);        %Photodiode Current
Epeak(i) = Ipeak(i)^2 * Tbit;     %Peak current energy
sigma(i)=sqrt(T_noise*Epeak(i)/2);
%standard deviation after receiver
threshold=0.5*Epeak(i);          %threshold level
for j=1 : nSignal;
receivedSignal(j) = randombinary(j)*Epeak(i)+ normrnd(0,sigma(i));
%matched filter output
end
% same of above cycle
Rx = zeros(1,nSignal);      %received signal inizialization
Rx(find(receivedSignal>threshold)) = 1; %threshold detection
[No_of_Error(i) simuBER(i)]=biterr(randombinary,Rx);
%matlab function
end

```

```
theorBER = qfunc(sqrt(SNR_e)); %theoretical formula of OOK BER

end
```

Appendix E (Function to QAM and QPSK)

```
function [im_qpsk,im_16qam,im_64qam, in] = QAM_and_Qpsk(SNRdb)
SNRdb=max(max(SNRdb));
%%% Modulator and Demodulator Objects %%%
h_qpsk=modem.pskmod('M',16,'phaseoffset',pi/16,'inputtype','bit');
g_qpsk=modem.pskdemod('M',16,'phaseoffset',pi/16,'outputtype','bit');
h_16qam=modem.qammod('M',16,'inputtype','bit');
g_16qam=modem.qamdemod('M',16,'outputtype','bit');
h_64qam=modem.qammod('M',64,'inputtype','bit');
g_64qam=modem.qamdemod('M',64,'outputtype','bit');
%%%%% TRANSMITTER
in=imread('4.2.03.tiff'); % image to be transmitted and
N=numel(in); % matlab code should be in same directory
in2=reshape(in,N,1);
bin=de2bi(in2,'left-msb');
input=reshape(bin',numel(bin),1);
len=length(input);
%%% padding zeroes to input %%%
z=len;
while (rem(z,2) || rem(z,4) || rem(z,6))
    z=z+1;
    input(z,1)=0;
end
input=double(input);
y_qpsk=modulate(h_qpsk,input);
y_16qam=modulate(h_16qam,input);
y_64qam=modulate(h_64qam,input);
ifft_out_qpsk=ifft(y_qpsk);
```

```

ifft_out_16qam=ifft(y_16qam);
ifft_out_64qam=ifft(y_64qam);

tx_qpsk=awgn(ifft_out_qpsk,SNRdb,'measured');
tx_16qam=awgn(ifft_out_16qam,SNRdb,'measured');
tx_64qam=awgn(ifft_out_64qam,SNRdb,'measured');

%%%%% RECEIVER

k_qpsk=fft(tx_qpsk);
k_16qam=fft(tx_16qam);
k_64qam=fft(tx_64qam);
l_qpsk=demodulate(g_qpsk,k_qpsk);
l_16qam=demodulate(g_16qam,k_16qam);
l_64qam=demodulate(g_64qam,k_64qam);
output_qpsk=uint8(l_qpsk);
output_16qam=uint8(l_16qam);
output_64qam=uint8(l_64qam);
output_qpsk=output_qpsk(1:len);
output_16qam=output_16qam(1:len);
output_64qam=output_64qam(1:len);
b1=reshape(output_qpsk,8,N)';
b2=reshape(output_16qam,8,N)';
b3=reshape(output_64qam,8,N)';
dec_qpsk=bi2de(b1,'left-msb');
dec_16qam=bi2de(b2,'left-msb');
dec_64qam=bi2de(b3,'left-msb');

BER_qpsk=biterr(input,l_qpsk)/len;
BER_16qam=biterr(input,l_16qam)/len;
BER_64qam=biterr(input,l_64qam)/len;
%%%%% Received image data
im_qpsk=reshape(dec_qpsk(1:N),size(in,1),size(in,2),size(in,3));

```

```
im_16qam=reshape(dec_16qam(1:N),size(in,1),size(in,2),size(in,3));  
im_64qam=reshape(dec_64qam(1:N),size(in,1),size(in,2),size(in,3));  
end
```